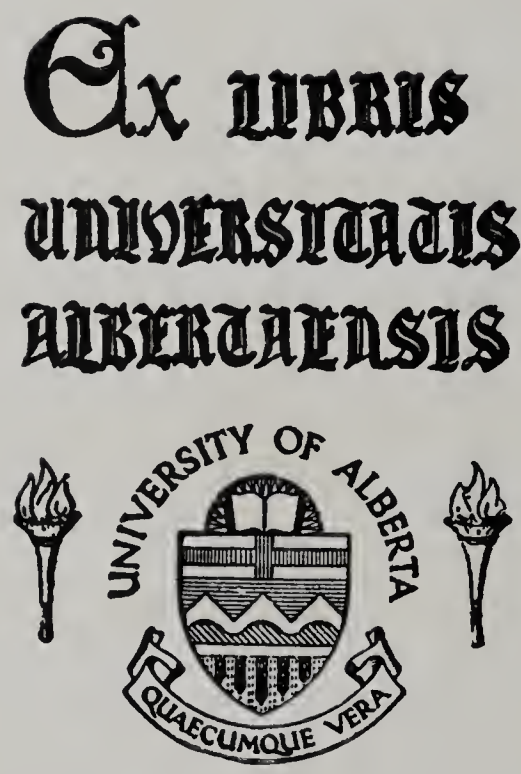

University of Alberta
Printing Department

THE UNIVERSITY OF ALBERTA

AN INVESTIGATION OF FATIGUE CRACK PROPAGATION IN MILD STEEL SHEET SUBJECTED TO CYCLIC BENDING

by

BRYAN R. LONG, B. Sc. (Alberta)

A THESIS

SUBMITTED TO THE FACULTY OF GRADUATE STUDIES

IN PARTIAL FULFILMENT OF THE REQUIREMENTS FOR THE DEGREE

OF MASTER OF SCIENCE

DEPARTMENT OF MECHANICAL ENGINEERING

EDMONTON, ALBERTA

June 1965

UNIVERSITY OF ALBERTA

FACULTY OF GRADUATE STUDIES

The undersigned certify that they have read, and recommend to the Faculty of Graduate Studies for acceptance, a thesis entitled "An Investigation of Fatigue Crack Propagation in Mild Steel Sheet Subjected to Cyclic Bending" submitted by Bryan R. Long in partial fulfilment of the requirements for the degree of Master of Science.

ABSTRACT

Tests were conducted to determine the rate of fatigue crack growth in terms of the applied stress and current crack length in mild steel sheet subjected to cyclic bending stresses, which were induced by resonant vibration. It was found that the rate of extension was proportional to the fourth power of the range of applied stress and was influenced by the value of the mean stress. It was also found that, for constant stress cycles, the rate of crack propagation was a constant; this was in agreement with the Weibull theory of crack propagation.

As a consequence of the tests it was found that a fatigue crack did not appreciably reduce the resonant frequency of the test beams until the crack had progressed most of the way across the specimen.

ACKNOWLEDGEMENTS

An expression of gratitude is extended to each of the following who contributed much to the thesis:

- Dr. D.G. Bellow for his helpful guidance in conducting the experiments and writing the thesis,

- Mr. R. Marak, Mr. W. Kell and Mr. H. Golls who were responsible for the experimental apparatus,

- Mrs. M. Faulkner for her excellent typing of the thesis,

- the National Research Council for the funds under grant no. A-2705, which were instrumental in the completion of the thesis.

TABLE OF CONTENTS

LIST OF FIGURES

NOTATION

k, K	Spring constants in Orowan model
P	Load applied to model
Δ	Extension of model due to load P
δ	Elongation of plastic region; later refers to amplitude of vibration of test specimens
T	"Stress" in plastic region
L	Total crack length in test specimen
N	Number of loading cycles applied to test specimen
C_1	Constant in Head theory
a	Width of plastic region in Head theory
C_2	Constant in Frost and Dugdale theory
$\overline{\nabla}$	Range of stress
N_s	Constant which depends on mean stress
K_t	Theoretical stress concentration factor
x	Ratio of crack length to specimen width in Weibull theory
C_3, β	Constants in Weibull theory
r	Radius of tip of crack
$\overline{\nabla}_e$	Endurance limit
b	Width of test specimen
$\overline{\nabla}_o$	Initial range of stress in a test

GENERAL PLAN OF THE THESIS

In Chapter I an introduction to the phenomena of fatigue and, in particular, fatigue crack propagation is given. The aims of the thesis are stated, together with some remarks which attempted to justify the investigation.

In Chapter II a model is presented which illustrates the qualitative aspects of fatigue crack growth. This is followed by a discussion of the existing theory of crack propagation. The possible application of this theory to the present problem is discussed.

Chapter III presents the details of the experimental methods employed in the investigation. Included are discussions of the apparatus, preparation of the test specimens, means of measuring crack length and determination of the stress levels.

Results of the various tests carried out are given in Chapter IV and a comparison of measured rate of crack propagation with that predicted by theory is made. Included are various observations made during the testing program.

In Chapter V conclusions are presented and possible practical applications of the findings are discussed. Also included are recommendations for further research.

Appendix A discusses fatigue crack propagation where the specimen is subjected to a discrete change in the applied stress level at some time during the test. Appendix

B includes a graph showing the measured decrease in natural frequency caused by a propagating crack. Details of the test equipment are presented in Appendix C.

CHAPTER I

INTRODUCTION

1.1 Introduction to the Problem

The propagation of fatigue cracks did not engage the interest of scientists and engineers until relatively recently, although the phenomenon of failure by fatigue was recognized as early as 1839 (1).* Early investigators were concerned with the number of loading cycles, at a given stress level, necessary to cause complete failure in a machine part or test specimen. No attempt was made to separate the problem of fatigue failure into the crack propagation phase and the crack initiation phase; this step is vital to gaining an understanding of the complete problem. Early tests were also conducted to find the level of stress to which a member could be subjected for any number of cycles without failure.

With advances in technology and in particular the introduction of the aircraft, the commonly used high factors of safety became unacceptable in many applications. Use of reduced safety factors increased the possibility of fatigue damage and led to the development of the "fail-safe" design concept in the aircraft industry. The development of the fail-safe design concept has been primarily responsible for

* Numbers in brackets denote references contained in the Bibliography.

the recent increase in interest in fatigue crack propagation.

1.2 Aim of the Thesis

Of the two phases of fatigue failure, this thesis is concerned with the crack propagation phase. The aim is to determine the rate of fatigue crack propagation in mild steel test specimens and to compare the experimental results with existing theory. The thesis is concerned with fatigue cracks caused by cyclic bending stresses and by combined cyclic bending stresses and static axial stresses.

The problem under consideration is representative of the case of sheet material subjected to resonant vibration, such as might be encountered in aircraft or in space vehicles.

It is in these same applications that the case of the superimposed axial stress will be found; for example, in the prestressed outer skin of an aircraft. A second example is in blading for turbines or compressors. In nearly all applications of this type this axial stress will be tensile since thin metal sheet can buckle under low compressive loading.

For all of the tests carried out for this thesis cracks were induced by cyclic bending stresses. In most of the recent work the practice has been to subject test specimens to axial loading only. There are many cases, however,

in which bending will be more representative of the actual situation, particularly where members are subjected to resonant vibration.

It should be pointed out that only the macroscopic aspects of fatigue crack growth were investigated. The microscopic aspect of fatigue is a complex problem in itself and is beyond the scope of this thesis.

1.3 Historical Review

Fatigue failure of metals was recognized as early as 1839 by Poncelet (1) who first introduced the term "fatigue". At this time it was commonly believed that fatigue damage occurred due to a recrystallization of the metal when subjected to shock and vibration. The first extensive investigations of fatigue failure were carried out by Wohler (1) who studied fatigue due to bending, axial loading, torsion and combined states of stress. These studies were carried out over a period from about 1850 to 1870. However, there was apparently little interest in the study of fatigue crack propagation until 1927 when Moore (2) measured crack growth in cylindrical test specimens subjected to rotary bending.

In 1936, de Forest (3) recognized the necessity of separating the problem of failure by fatigue into the crack initiation and crack propagation phases. De Forest measured the rate of crack propagation in cylindrical steel specimens

having various surface finishes and subjected to rotary bending. It was found that, for a given loading, crack initiation was essentially a function of surface condition, while crack propagation was independent of surface condition.

Orowan (4) in 1939 assumed that the stress distribution in any material was not completely homogeneous due to the presence of micro cracks, flaws and structural inhomogeneities. These cause stress concentration effects which, if of sufficient magnitude, lead to progressive work hardening and eventually to local fracture, thereby initiating a crack. He suggested that the fatigue crack propagates in the same manner, with the stress concentration effect provided by the existing crack. Contrary to some other findings, his theory predicted that the rate of crack propagation was dependent on stress range only. (The range of stress refers to the magnitude of the difference between the maximum and minimum stresses in a loading cycle).

In 1946, Bennett (5) measured crack growth rates in cylindrical steel specimens in rotary bending and found that the crack length increased exponentially with the number of loading cycles. Although this was in agreement with a later theory (10), these measurements could not be regarded as substantiation of the theory because of the complexity of the stress distribution.

Head (6) in 1953 analyzed fatigue crack propagation

with the use of a model which was essentially the same as that proposed by Orowan (4). An expression was obtained for the rate of crack extension in terms of the current crack length, applied stress, material properties and the size of the plastic zone at the crack tip. It was assumed that the size of this zone remained constant as the crack extended.

Weibull (7,8) in investigations in 1954 and 1956, attempted to account for the increase in applied stress caused by a fatigue crack, under axial loading conditions, by assuming that the stress increased in proportion to the decrease in net area. He conducted tests in which the applied load was continuously reduced such that the applied stress was constant. The corresponding rate of crack growth was found to be constant. Some doubt has been expressed (10) concerning the validity of Weibull's assumed increase in stress.

In 1956, Frost and Phillips (9) found that non-propagating cracks could be formed in specimens of mild steel and aluminum stressed below the endurance limit of the material.

Frost and Dugdale (10) in experiments in 1958 found that the size of the plastic region at the tip of a propagating crack in mild steel was proportional to the current length of crack for crack lengths of up to at least one quarter of the gross section width. Their measurements indicated that the rate of crack propagation in mild steel

was independent of the applied mean stress, being a function of the stress range only. For aluminum they found that the rate of extension was influenced by both mean stress and stress range.

Liu (11) in 1961 developed an expression for the rate of crack propagation in thin sheet using a dimensional analysis procedure. The same relation had been suggested earlier by Frost and Dugdale (10), but was presented without proof. Taking measurements of the rate of crack extension in sheets of 2024-T3 aluminum alloy under axial loading, Liu determined the dependence of the rate of growth on stress range and mean stress. In a theoretical investigation in 1963 Liu (12), assuming that a critical amount of hysteresis energy absorption is the criterion for crack extension, found the rate of crack propagation was proportional to the square of the stress range. However in a discussion of this paper, Paris and Erdogan (13) suggested that the index could be three or four based on actual measurements.

Working with aluminum alloys, Hudson and Hardrath (14) in 1963, found measurable increases in crack length under single loading cycles which were representative of gust loadings on aircraft structures and that in these cycles the peak stress had a greater influence on the amount of growth than did the stress amplitude. In an investigation in 1961, Hudson and Hardrath (15) measured

crack growth in axially loaded aluminum sheet. Tests were run to determine the effect of a non-constant stress level by varying the applied load at some time during the life of a specimen. It was found that significant delays in crack extension occurred when the change in the applied stress was from a high to a low value.

In discussing (16), Hardrath pointed out that this delay only occurred when the increment of stress was sufficiently large.

Weibull (16), 1963, found three stages in the propagation of a fatigue crack under axial loading, corresponding to different modes of failure; namely, tension, single shear and double shear. He noted that the parameters which influence the rate of growth may be different in each of the modes and it is therefore necessary to know the particular mode of failure when comparing various measurements of crack propagation.

1.4 General Remarks on Fatigue

Before proceeding with a description of the mechanism of fatigue crack propagation, it will be of interest to discuss some of the factors which are commonly accepted as influencing fatigue crack initiation and/or propagation.

Fatigue failure is produced by progressive fracture leading from points of high stress concentration or from points of weakness in the material when the applied fluctuating stress is of sufficient magnitude.

Examination of test specimens with an electron microscope has shown that in the early stages of loading inelastic action occurs, resulting in permanent slip lines (17). Continued loading causes voids of microscopic magnitude to be developed. These voids gradually grow and join together to form a microscopic crack, often quite early in the life of the specimen. Under continued cyclic loading this microscopic crack can grow to eventually cause catastrophic failure.

Once formed, a fatigue crack propagates in a direction which is generally normal to the direction of the maximum applied tensile stress, although it may deviate locally around regions of high strength. The propagation is usually transgranular. Since the initiation, and possibly the propagation, of fatigue cracks is influenced by local weaknesses in the metal, it is not surprising that a wide variation in fatigue properties can be obtained from tests of apparently identical specimens. This introduces the necessity of using statistical methods when analyzing results of fatigue tests with the aim of determing fatigue characteristics.

Some of the more important factors which influence the fatigue strength of a metal part are:

(a) inhomogeneity in the metal

(b) size of member

(c) shape of member

(d) speed of testing

(e) surface finish

(f) temperature and humidity

(g) residual stresses.

Probably the most important of these factors from an engineering view point is (c). Variations in shape, holes, fillets, keysways, etc. can introduce large stress concentrations in a part, greatly increasing the susceptibility to fatigue crack initiation.

It has been noted (Section 1.2) that the surface finish can have an important effect on crack initiation but does not normally influence propagation. Surface roughness can cause a significant stress concentration effect, leading to initiation of a crack. Once initiated, however, the crack propagates due to the large stress concentration at the tip of the crack and is apparently not influenced by small surface irregularities.

The effect of the rate of testing on the fatigue strength of a test specimen has been investigated and, although there is some disagreement, it was suggested by Marin (17) that there is little effect in the range from 3 to 100 c.p.s. Lachenaud (19) found that the rate of crack growth increased rapidly in changing the test frequency from 30 c.p.s. to 1/3 c.p.s.

With regard to (b), there is some agreement that an increase in the size of a member, all other parameters being constant, will cause a decrease in fatigue strength (17). This can be explained on the basis of a larger specimen containing more points of weakness at which a crack might be initiated.

CHAPTER II

MECHANISM OF FATIGUE CRACK PROPAGATION

2.1 Orowan Model

In order to illustrate the mechanism of fatigue crack propagation it is convenient to employ a mechanical model of an idealized material which is composed of a homogeneous elastic region surrounding a homogeneous plastic region. For a fixed load applied to a specimen of this material, the stress in this plastic zone depends on the amount of plastic strain in the zone. This situation arises since plastic deformation of this element causes an increase in elastic strain (and consequently stress) in the surrounding elastic medium. Because of the increased stress in the elastic region, there must be a decrease in the stress in the plastic element, since the total load remains constant.

The above characteristics are contained in the mechanical model of this material as shown in Figure 2.1. In the model the plastic element marked A represents the plastic zone in the material while the two springs of constant K represent the surrounding elastic material. The spring of constant k represents the constraint of the surrounding elastic material on the plastic element.

For any total load P there is an elongation Δ of the system which remains unaltered regardless of how much

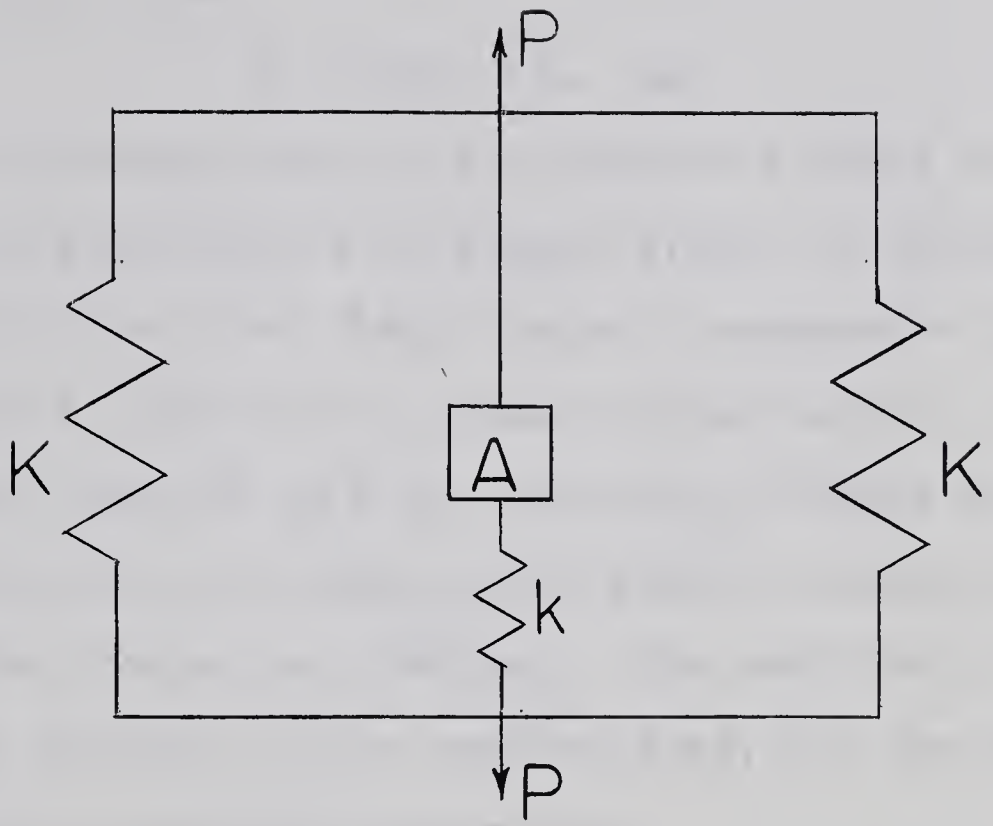

Figure 2.1. Model of Idealized Material

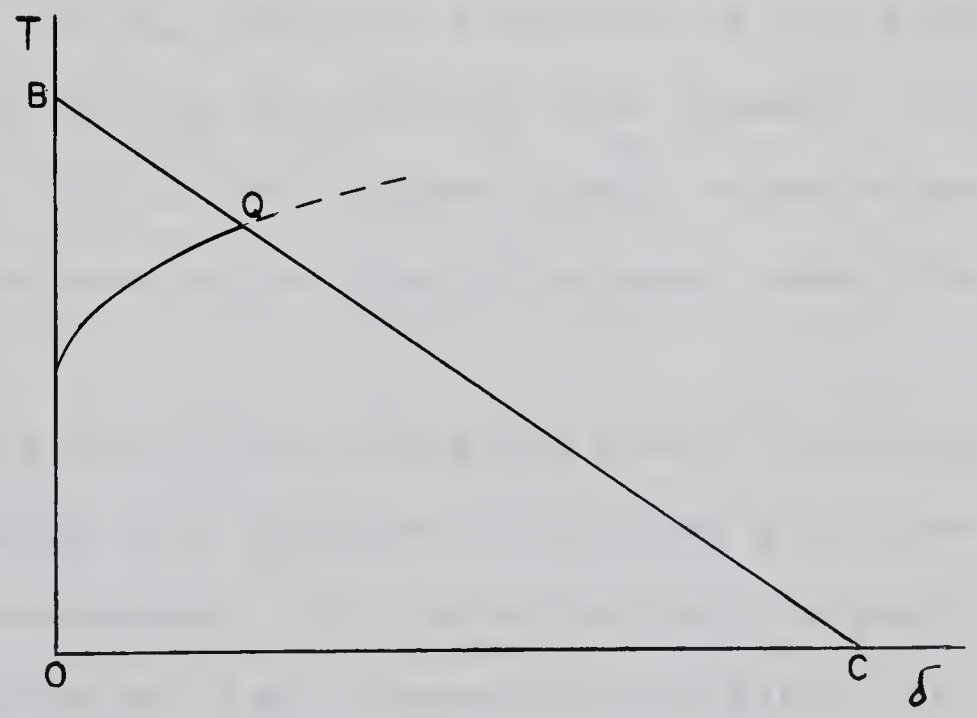

Figure 2.2. Stress-Strain State in Plastic Element

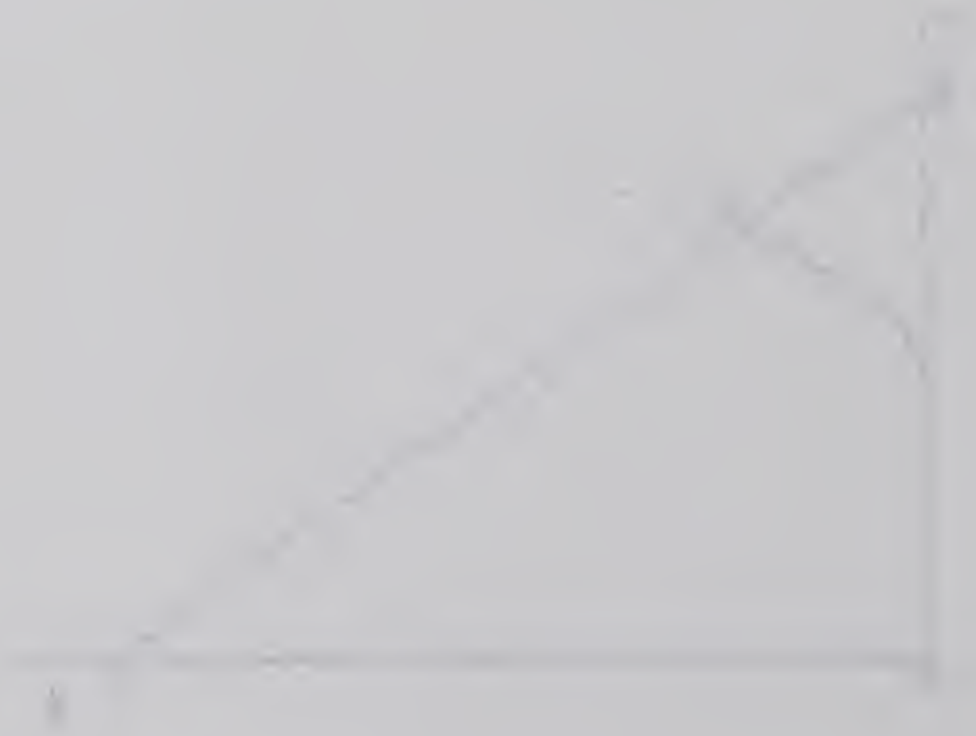

A yields since $K \gg k$. If the load in A is T and the elongation is δ, then

$$T = k(\Delta - \delta). \quad (a)$$

Thus if no yielding occurs in the plastic element the load in it is $k\Delta$ (Point B in Figure 2.2). If the element yields freely ($T = 0$ and $\delta = \Delta$) point C represents the "stress-strain" state in the element after loading. Since T is a linear function of δ the line BC in Figure 2.2 represents the state of stress in the plastic element for an intermediate amount of yielding. The position of the line BC is a function of the applied load, but the slope is influenced by material properties.

When the elastic material containing the plastic element is loaded the stress-strain state in the element follows the curve OQ, which is a segment of the stress-strain diagram for the material in that element. The intersection of BC and the stress-strain curve represents the state of stress in the plastic element under the applied load P.

With the aid of the foregoing model the response to cyclic loading of a specimen containing a fatigue crack will now be considered. In this situation the plastic element is caused by high stresses in the region of the crack tip.

Figure 2.3 shows the response of the idealized material to completely reversed cyclic loading (i.e.

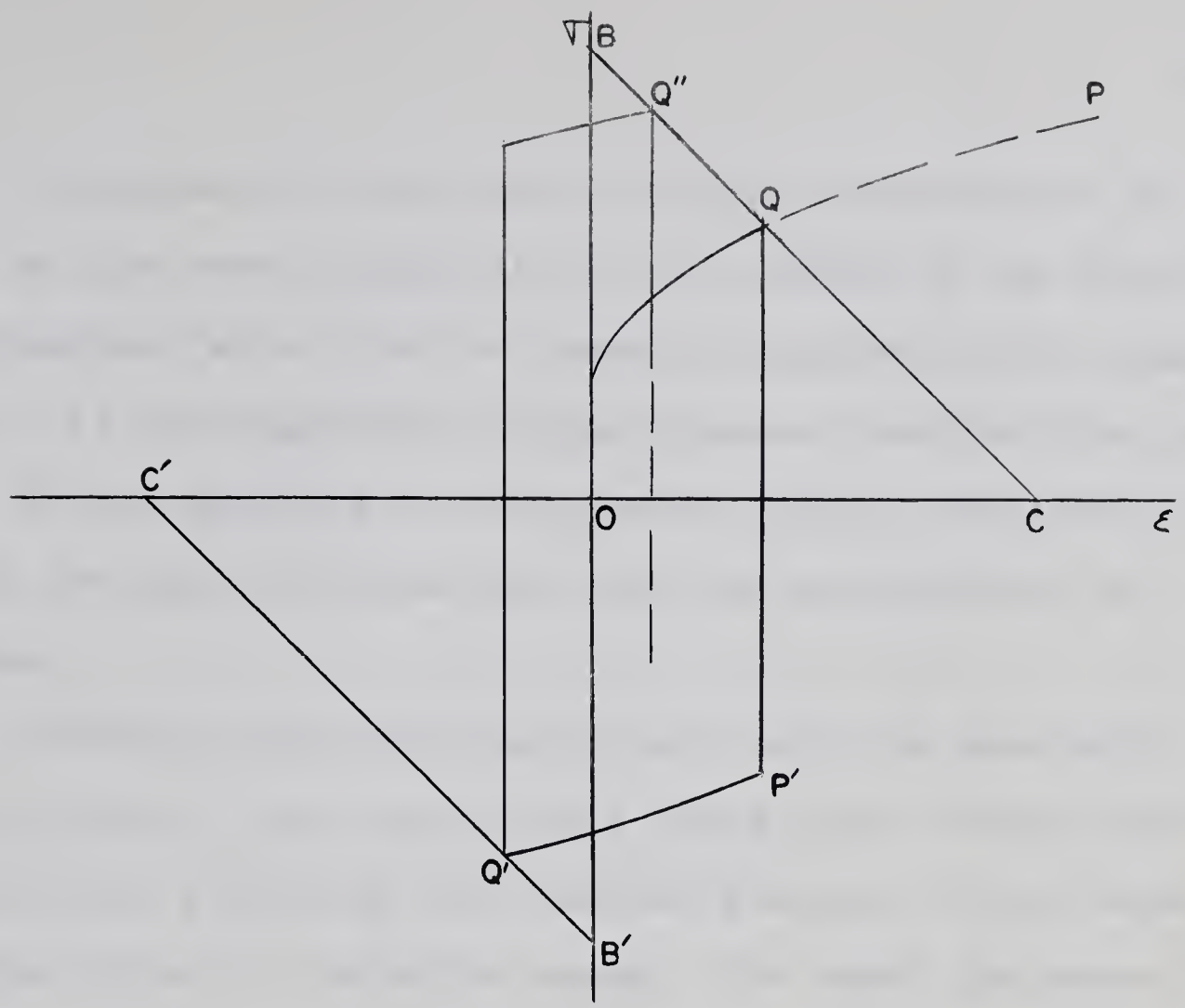

Figure 2.3. Increase in Stress in Plastic Element under Cyclic Loading.

mean stress is zero). The line BC is the same as that shown in Figure 2.2 while B′C′ is the same line for compressive loading. During the first half cycle of loading, which is assumed to be tensile, the stress rises to Q in the same manner as in Figure 2.2. When the load reverses direction, the stress-strain state in the plastic element follows the path QP′Q′. The portion P′Q′ of this curve is the appropriate portion of the stress-strain curve OQP which lies to the right of Q. Under the next load reversal the stress reaches Q″. In this way the stress eventually becomes equal to the value at B, say σ_B.

The stress σ_s represents the full concentration of stress at the crack tip; that is, σ_s is equal to the stress concentration factor for the crack multiplied by the nominal stress. If the magnitude of σ_s is greater than the fracture stress of the material in the plastic region, fracture of some of the material will occur and the process will be repeated.

Orowan's model is in agreement with the generally accepted theory that crack growth takes place through progressive work hardening and eventual fracture of the material near the tip of the existing crack. The model indicates that a fatigue crack extends in a series of steps rather than in a continuous manner (i.e. rather than extending a finite amount under each loading cycle) unless the applied nominal stress is sufficiently large. If this stress is of sufficient magnitude the stress at point Q (or at Q′) in Figure 2.3 could be in excess of the fracture stress.

In support of this last point, Hudson and Hardrath (14) found measurable increases in crack length in axially loaded aluminum sheet under single loading cycles. However, in other tests average rates of extension of the order of one atom per stress cycle have been observed. It does not seem likely that the propagation would be continuous at this rate of growth. The possible consequences of the crack propagating in a discontinuous manner are not fully understood , but this might introduce some error into present

theories which assume the process is continuous.

It should be noted that a material which exhibits a Bauschinger effect will not respond to reversed cyclic loading exactly as indicated by Figure 2.3. The actual stress-strain path followed by such a material during the compressive part of the first loading cycle will lie above PQ. According to Orowan the Bauschinger effect tends to reduce the rate of crack propagation.

2.2 Theory of Fatigue Crack Propagation

2.2.1 Head Theory

Head (6) used a model such as that described in Section 2.1 to develop a quantitative expression for the rate of crack growth in terms of the crack geometry and the applied stress. Material in the plastic region A at the crack tip was assumed to be rigid-plastic work-hardening and the size of the zone was assumed constant. Head considered the response of a typical element in the plastic region to cyclic loading and, through a rather complicated analysis, found that

$$\frac{dL}{dN} = \frac{C_1 L^{3/2}}{a^{1/2}} \qquad (b)$$

where "a" was the width of the plastic region and C_1 was a constant which contained the applied stress and the material stress-strain properties. It was assumed in the analysis that the plate was of infinite width and that the

amplitude of the nominal stress was constant.

In attempting to justify his theory, Head used measurements taken by Moore (2), De Forest (3) and Bennett (5) all of whom measured crack growth in cylindrical specimens in rotary bending. Head found that $L^{-1/2}$ plotted versus N, the number of stress cycles, gave straight lines, as predicted by his analysis.

It can not be concluded that these measurements confirm this theory as the region of the crack in this configuration is subject to a complicated tri-axial stress system. Furthermore, it has been shown that the plastic region at the crack tip does not remain constant in size (10). If Head's analysis is modified with the assumption that the size of the plastic region is proportional to the crack length, then the result is in partial agreement with the theory described in the next section. The parameter C_1 is a rather complicated function of the applied stress and does not appear to agree with experimental evidence (10,13) nor with other theories (12).

2.2.2 Frost and Dugdale Theory

It was suggested by Frost and Dugdale (10) that the rate of crack propagation in thin sheet material is proportional to the crack length, i.e. that

$$\frac{dL}{dN} = C_2 L \qquad (c)$$

in which the factor C_2 is a constant for a given range of stress and a given mean stress. This assumed that the configuration of stress and strain remained geometrically similar as the crack propagated, but a complete proof of the expression was not presented.

However, Liu (11) obtained the same expression for the rate of crack propagation in a semi-infinite sheet using a dimensional analysis approach. In deriving this expression it was assumed that plane stress existed and that geometric similarity was maintained as the crack propagated. This latter condition is satisfied in an infinite plate or in a plate whose width is large compared with the crack length providing the applied stress remains constant.

This theory predicts that the rate of crack propagation increases with increasing crack length when the applied stress is constant. This would mean that the stress at the crack tip is increasing, i.e. that there is an increasing stress concentration factor. Since the stress concentration factor is influenced by the length of the crack, this could in fact occur.

It was suggested by Frost and Dugdale that the factor C_2 can be represented by

$$C_2 = \frac{\bar{\sigma}^n}{N_s} \quad (d),$$

where $\bar{\sigma}$ is the stress amplitude. The value of n is a material property, while N_s may be influenced by the

mean stress. On the basis of measurements of crack growth in aluminum and mild steel, Frost and Dugdale found n = 3.

Liu (12) suggested that n = 2 based on a theoretical analysis (See Section 1.4), while Paris and Erdogan (18) suggested n = 4 based on experimental evidence.

2.2.3 Weibull theory

Weibull (16) argued that the rate of fatigue crack propagation is determined by the applied stress based on the remaining area, regardless of the existing crack length. That is, for a given stress amplitude and mean stress, the rate of crack growth is constant.

In support of this proposal, Weibull suggested that the stress concentration factor at the crack tip in an infinite plate can be represented by

$$K_t = 1 + 2(L/r)^{1/2} \quad (e),$$

where r is the radius of the root of the crack. If the ratio L/r is constant and the nominal applied stress is constant, then the stress at the crack tip will be constant. As long as the preceding condition exists, it is reasonable that the rate of crack propagation should not vary.

In this theory it was also suggested that the rate of crack growth is influenced by the specimen width, so that the basic formula for crack propagation was presented as

$$dx/dN = C_3 (\sigma_x - \sigma_e)^{\beta} \quad (f),$$

where C_3 and β are material constants, x is crack length to

specimen width ratio, σ_x is the nominal stress amplitude, and σ_e is the endurance limit. Weibull found that the parameters C_3, β and σ_e in this equation varied with a change in the mode of failure (See Section 1.4).

There is some evidence to support Weibull's suggestion that the radius r is not necessarily a material constant. Frost and Phillips (9) observed non-propagating cracks in mild steel and aluminum specimens stressed below their endurance limits. Since this was observed for constant stress amplitudes, the stress concentration factor must have decreased to a point where the stress at the crack tip was less than the fracture stress. Based on Equation (e) this indicates an increasing value of r.

2.3 Application of Theory

2.3.1 Crack propagation in bending

The theories in Sections 2.2.1 and 2.2.2 were developed under the assumption that a plane stress condition exists in the region of a propagating crack, a situation which would likely be realized in thin specimens subjected to axial loading.

However, when the propagation of a fatigue crack is caused by bending stresses it is less likely that plane stress conditions will be approached. Fibres on the outside of the specimen will be the first to exceed the yield

stress and deform plastically. Not only will this deformation be constrained by surrounding elastic material, but also by neighbouring fibres, i.e. fibres nearer the neutral axis. This constraint will induce transverse shearing stresses which may alter the form and/or size of the plastic region at the crack tip as compared to axial loading with an equal maximum stress.

In addition to these stresses, there will be transverse shearing stresses due to the nature of the loading. It is not known whether the magnitude of these stresses will be significant when compared to the bending stresses.

It follows from the above considerations that the crack length will decrease in going from the outside surface toward the neutral axis. It is also expected that cracks will form at each of the outside surfaces of the beam and that these will propagate independently of each other.

2.3.2 Increasing nominal stress

In axially loaded test specimens subjected to a constant load amplitude the nominal stress range, based on the net remaining area, increases as the crack extends. However, when considering a theory of crack propagation it is more convenient to have a constant stress range in order to reduce the number of variables involved. For this reason, some investigators (10,11) used wide sheets of material and measured crack growth over a small portion of

the total width. The assumption was made that the relatively small length of crack did not influence the nominal stress amplitude at the test section.

Weibull (16) disagreed with this last assumption. When measuring crack growth due to axial loading he reduced the amplitude of the applied load such that the stress based on the remaining area was constant.

In the problem under consideration in this thesis the non-constant nominal stress amplitude arises due to changes in the normal mode of vibration of the test specimens. The existence of a fatigue crack across a section will decrease the stiffness at that section and can therefore be expected to affect the nominal stress range, as defined in terms of curvature at the test section. An investigation of the amount of this effect for the beam configurations used in the testing program is presented in Chapter IV.

2.4 Effect of Mean Stress

In the case where a specimen is subjected to bending stresses only, the average stress at any point in the member over a cycle of loading is zero. Should the member have a superimposed axial load this will not be the case and some change in the crack propagation curve (i.e. crack length vs loading cycles) may occur.

This can be shown by considering a test specimen

under a constant maximum stress but with an increasing mean stress. In the limit, as the mean stress becomes equal to the maximum, the rate of crack growth must become zero, since this is merely static loading (providing the static loading causes a stress less than the fracture stress). On the other hand, for a given mean stress with an increasing stress range the rate of growth will eventually become infinite. Thus it is reasonable to expect that the rate of crack propagation is influenced both by mean stress and stress range. It follows, for a given maximum stress, that the rate of propagation is reduced for an increase in mean stress, while for a given range of stress the rate of growth increases with an increase in mean stress.

CHAPTER III

EXPERIMENTAL PROCEDURE

3.1 Test Series A

The first phase of the experimental investigation was the determination of the rate of fatigue crack extension in mild steel sheet for various ranges of applied stress with zero mean stress. Test specimens were cut from hot rolled mild steel sheet having a nominal thickness of 0.110 in. Specimen configuration and method of clamping are shown in Figure 3.1 and Figure 3.2. Properties of the material, whose ASTM designation is A-242, are listed in Figure 3.3. Mechanical properties were determined from a series of tensile tests, from which average results are presented. Figure 3.4 shows the determination of the elastic modulus.

All edges were machined and the stress raisers were cut with a milling cutter. Roots of the notches which had a 1/16 in. radius, were inspected visually and, when necessary, buffed lightly to obtain a smooth contour. The fact that this procedure may not have ensured completely uniform notches was of no consequence since it was assumed the notch had no influence on the crack propagation (3). The surface across which the crack was expected to propagate was polished lightly with a dressed wheel. It is shown by de Forest (3) that this will not affect the crack growth.

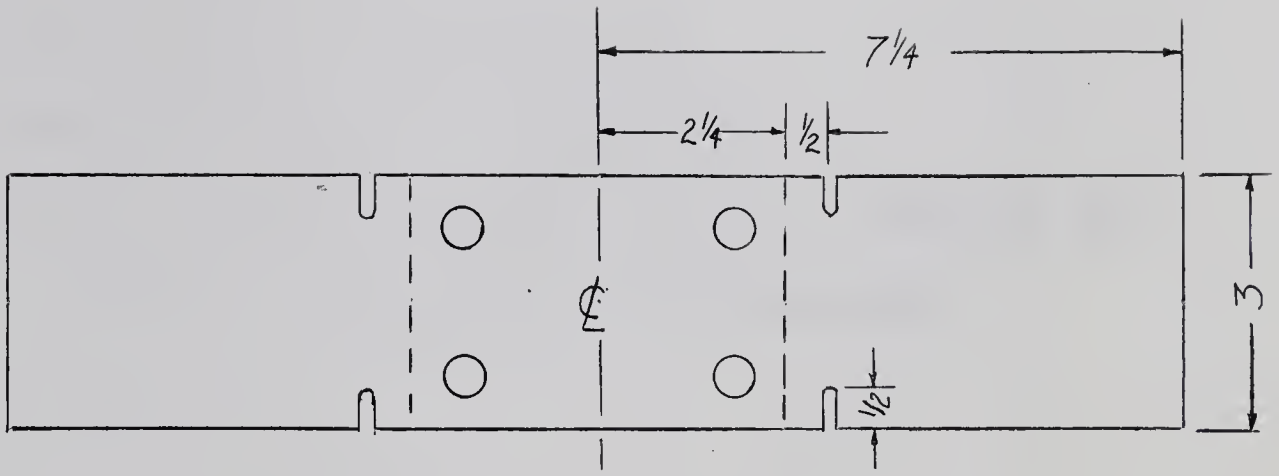

Figure 3.1 Specimen Configuration for Series A Tests

Figure 3.2. Test Specimen and Mounting Jig for Series A

Mechanical properties (measured):

$E = 30 \times 10^6$ psi

$\nu = 0.29$

Yield stress = 62,400 psi

Ultimate stress = 84,600 psi

Fracture stress (tensile test) = 153,000 psi

(Based on cross section at failure)

Chemical composition:*

C - 0.12%

P - 0.05 - 0.12%

S - 0.04% max.

Mn - 0.75%

Si - 0.20 - 0.45%

Cu - 0.30 - 0.60%

Cr - 0.30 - 0.60%

Ni - 0.30 - 0.60%

Figure 3.3 Mechanical Properties and Chemical Composition of Test Steel

* Data supplied by Steel Company of Canada

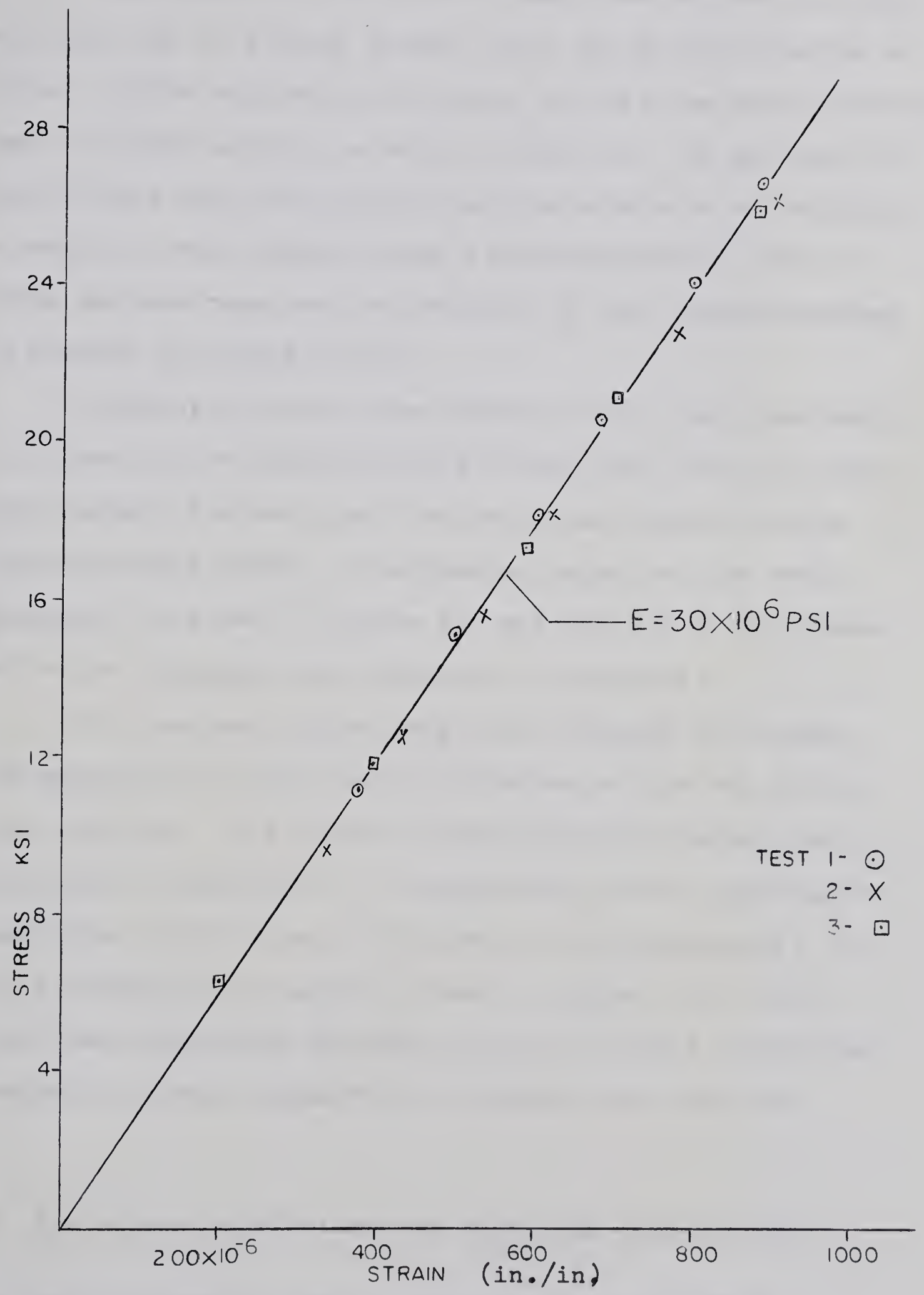

Figure 3.4 Determination of Elastic Modulus for Test Material

The extent of the crack at any time was easily found with the use of a glass prism, which had a magnification of five. A grid scribed on the prism allowed the direct measurement of crack lengths to within $\pm$0.004 in. In any case in which there was doubt concerning the existence or length of a crack, it was checked using a dye-penetrant.* Use of these methods required interruption of the loading program to measure the crack length.

Bending stresses were induced in the test specimens by vibrating the specimen and its mounting jig at the lowest resonant frequency of the beam on an Unholtz-Dickie electrodynamic shaker. The general layout of the test equipment is shown in Figure 3.5 and details of the shaker and other equipment are presented in Appendix C.

The desired stress range was obtained by setting the appropriate amplitude of vibration at the end of the test specimen. The method of adjusting this amplitude is discussed in Appendix C. A calibration curve relating the amplitude of vibration of the end of the specimen, δ, to the applied stress range is shown in Figure 3.6. This curve was determined through the use of bonded electrical resistance strain gauges** on a typical test specimen.

* Spot-Check manufactured by Magnaflux Corporation.

** Manufactured by Budd Instruments, type C6-181-E.

Clamped in front of, but isolated from, the test specimen was a piece of clear lucite on which a grid had been scribed as shown in Figure 3.2. During a test the amplitude of the specimen was observed through this grid using a ground glass screen on the back of a 4 in. x 5 in. Graflex camera. The grid and specimen were illuminated with a stroboscopic light system, the details of which are discussed in Appendix C. The smallest increment on the scaled grid was 0.020 in., so that the double amplitude of vibration was measured to within $\pm$0.020 in. The double amplitude for the set of tests was never less than 0.50 in. so that the maximum error in this quantity was less than $\pm$ 5 per cent.

Probably the greatest disadvantage in this arrangement was that the apparatus required constant monitoring by the operator. The existence of a fatigue crack caused changes in the natural frequency of vibration (see Appendix B) and consequently in the amplitude, so that the shaker frequency had to be reduced as the crack progressed. However, this decrease was small for crack lengths of less than half the specimen width, thus reducing the possiblility of error due to an unobserved change in amplitude.

In spite of these disadvantages, it was believed that this system of establishing the desired stress range was superior to the use of strain gauges since this system was simpler and faster to use, while being just as accurate.

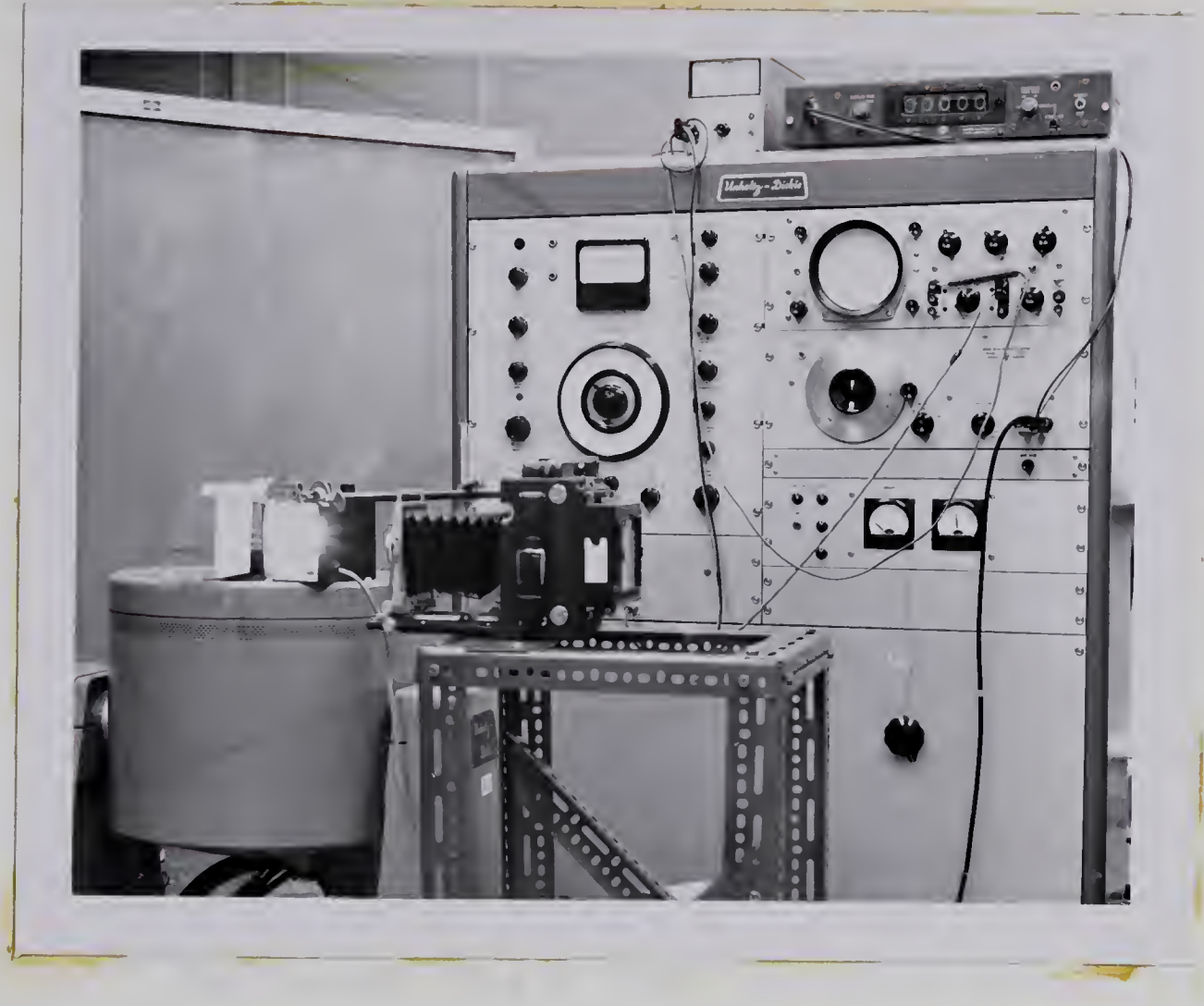

Figure 3.5. General View of Test Equipment

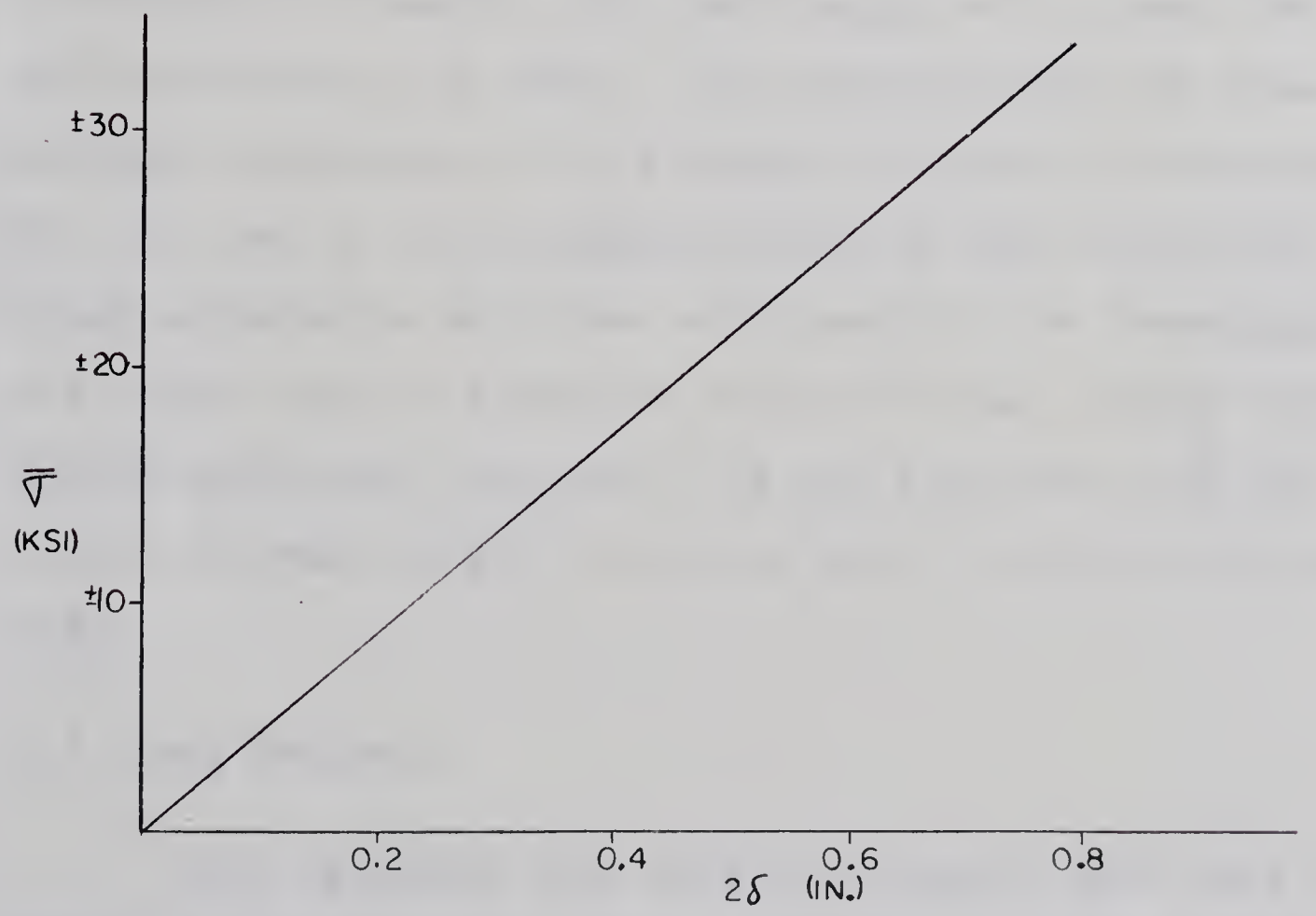

Figure 3.6. Calibration Curve for Cantilever Apparatus

The number of loading cycles applied were recorded on a General Radio digital frequency meter which can be seen in the upper right hand corner of Figure 3.5.

No correction was made to account for the fact that the built-in end of the cantilever was vibrating, since its amplitude was always less than 0.010 in. for these tests. The shaker table displacement was determined from an accelerometer mounted on the armature of the shaker (see Appendix C) which read out the peak-to-peak acceleration of the table.

When conducting a test, the specimen was subjected to several thousand cycles of loading (depending on the expected rate of propagation) and then the loading was interrupted to measure the crack length or to check for the initiation of a crack. This procedure did not allow accurate measurement of the number of cycles to initiation, but this was of no consequence since it was the rate of crack propagation which was of concern in the investigation. The method used to establish curves of crack length versus stress cycles was believed to be quite accurate for L/b (ratio of crack length to section width) between 0.10 and 0.80.

3.2 Test Series B

Test specimens with built-in supports were used to obtain a non-zero mean stress. This was done by building a jig with an adjustable span length as shown in Figure 3.7.

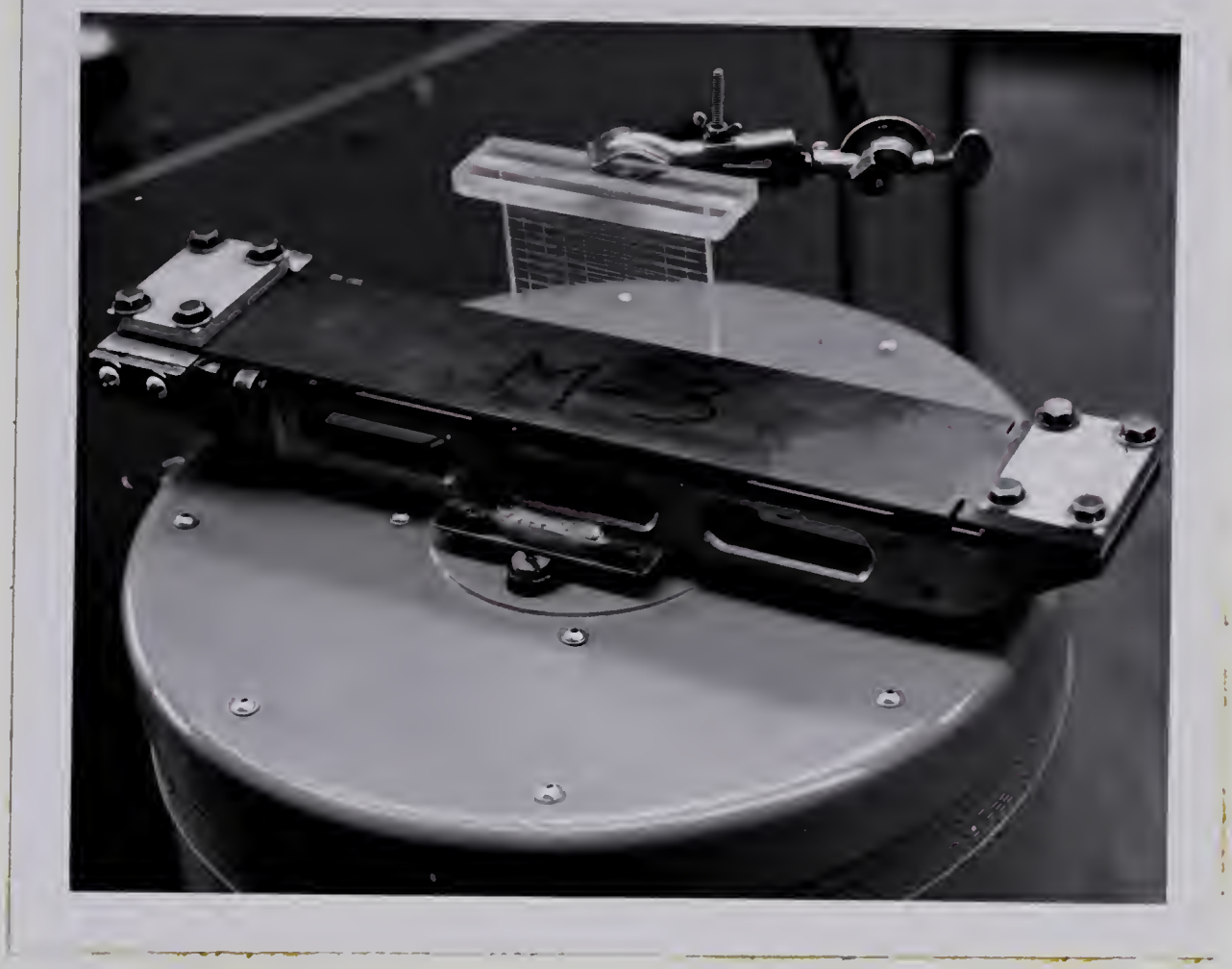

Figure 3.7. Test Specimen and Mounting Jig for Series B

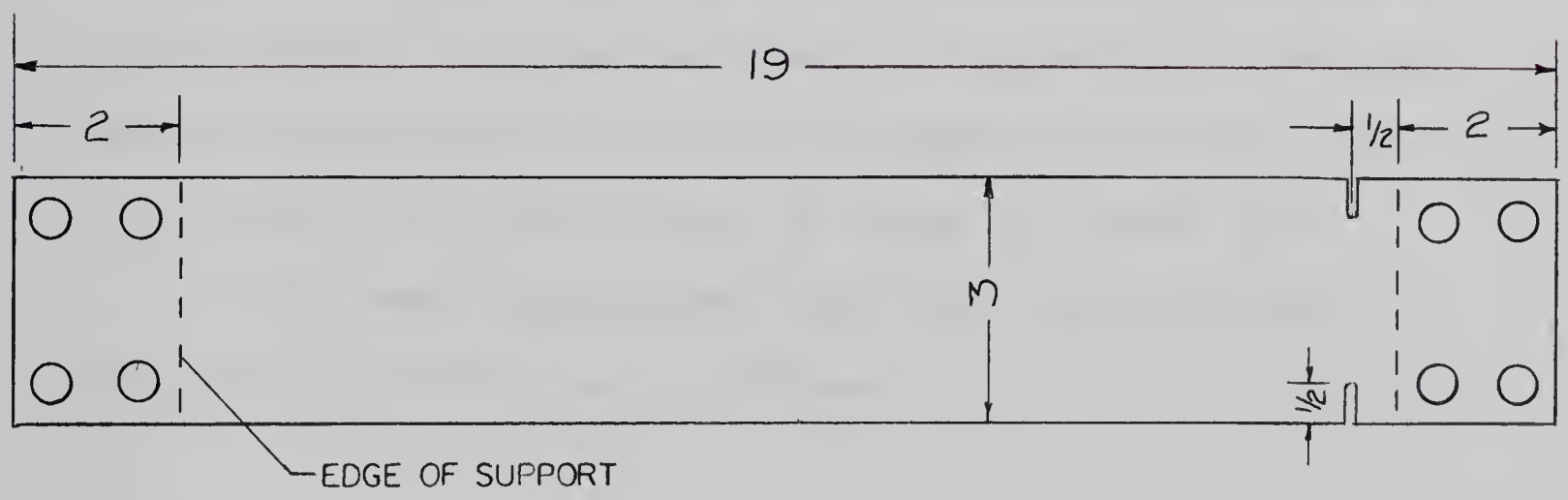

Figure 3.8 Specimen Configuration for Series B

Strain gauges, arranged in a Wheatstone bridge circuit to measure direct strains only, were used to indicate when the desired mean stress was reached and to monitor this stress throughout the test. With this apparatus it was possible to obtain mean stresses of up to 9,000 psi. based on the reduced area of the test section.

Beams vibrated in the built-in configuration theoretically have a non-zero mean stress even when no static axial load is applied due to elongation of the beam in the deflected position. Data from strain gauges applied to test specimens indicated this stress was small; certainly less than 500 psi. in all cases, and it was subsequently ignored.

Test beams were cut from the same material as those in Section 3.1 and prepared in the same manner, except for the difference in shape as shown in Figure 3.8. The calibration curve relating the double amplitude of the beam centre with the stress range is shown in Figure 3.9.

The remaining apparatus and the test procedure was identical with that in Series A.

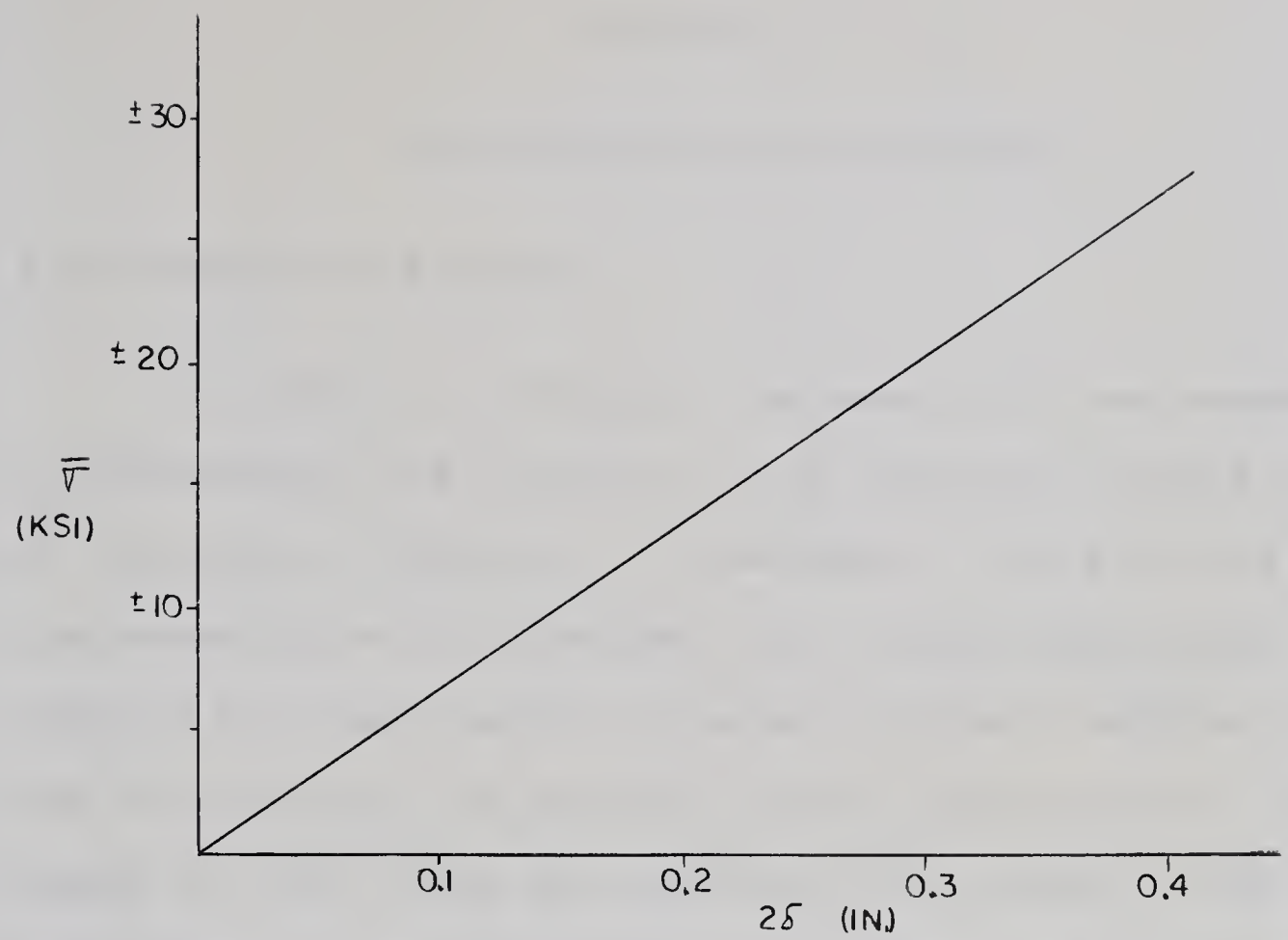

Figure 3.9 Calibration Curve for Fixed-Ended Apparatus

CHAPTER IV

TEST RESULTS AND DISCUSSION

4.1 Results of Series A

In order to interpret the results it was necessary to investigate the influence of an existing fatigue crack on the mode of vibration of the beam. This was done by instrumenting a test specimen with bonded electrical resistance strain gauges to measure dynamic bending strains and then testing the specimen in the usual manner. Any change in mode shape was detected by a change in the strain amplitude. It was found that the curvature at the test section was nearly constant* for values of L/b up to 0.5 and then started to increase as shown in Figure 4.1. (L/b is the ratio of total crack length to net specimen width at the test section.)

Results of tests conducted are presented in Figures 4.2, 4.3 and 4.4 and the curves are reproduced in Figure 4.5 to illustrate the comparison between the tests. Each of the Figures 4.2, 4.3, 4.4 represents a set of tests in which the actual maximum amplitude of vibration of the specimen was held constant throughout the test. Individual

* Checks revealed that there might have been a slight increase in the nominal stress range as L/b increased from zero to 0.5. However, if it existed this increase was small enough that the strain gauge network did not accurately indicate its magnitude.

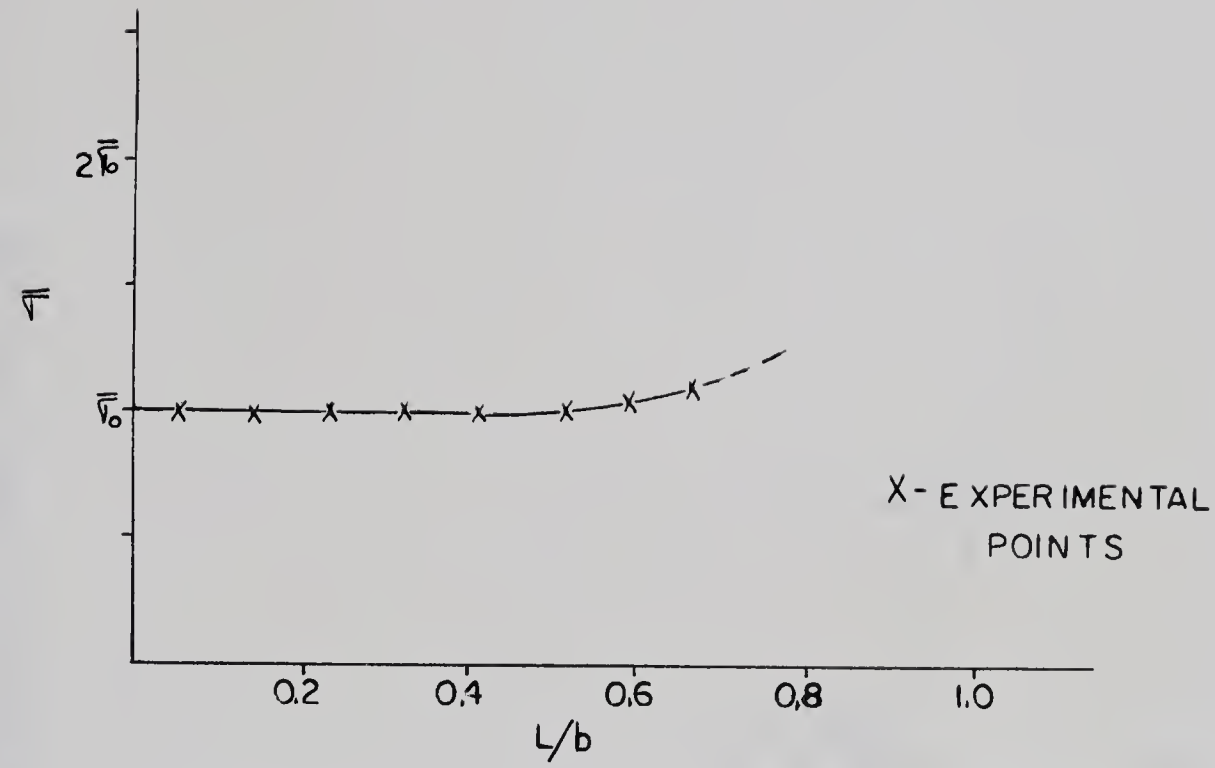

Figure 4.1 Effect of Fatigue Crack on Nominal Stress Range

test points at various crack lengths are shown to indicate the amount of scatter encountered and the solid curve is drawn through the arithmetic average of these points.

It is likely that a portion of the scatter encountered was due to variation in the number of cycles to initiate a crack at a particular stress level. Extrapolation of individual test curves back to a crack length of zero indicated that this was true. Figure 4.2 indicates the above quite clearly; with the exception of two tests the rate of crack extension appears to be quite uniform among the tests, yet there is a significant amount of scatter present. No attempt was made to eliminate the scatter from the initiation phase

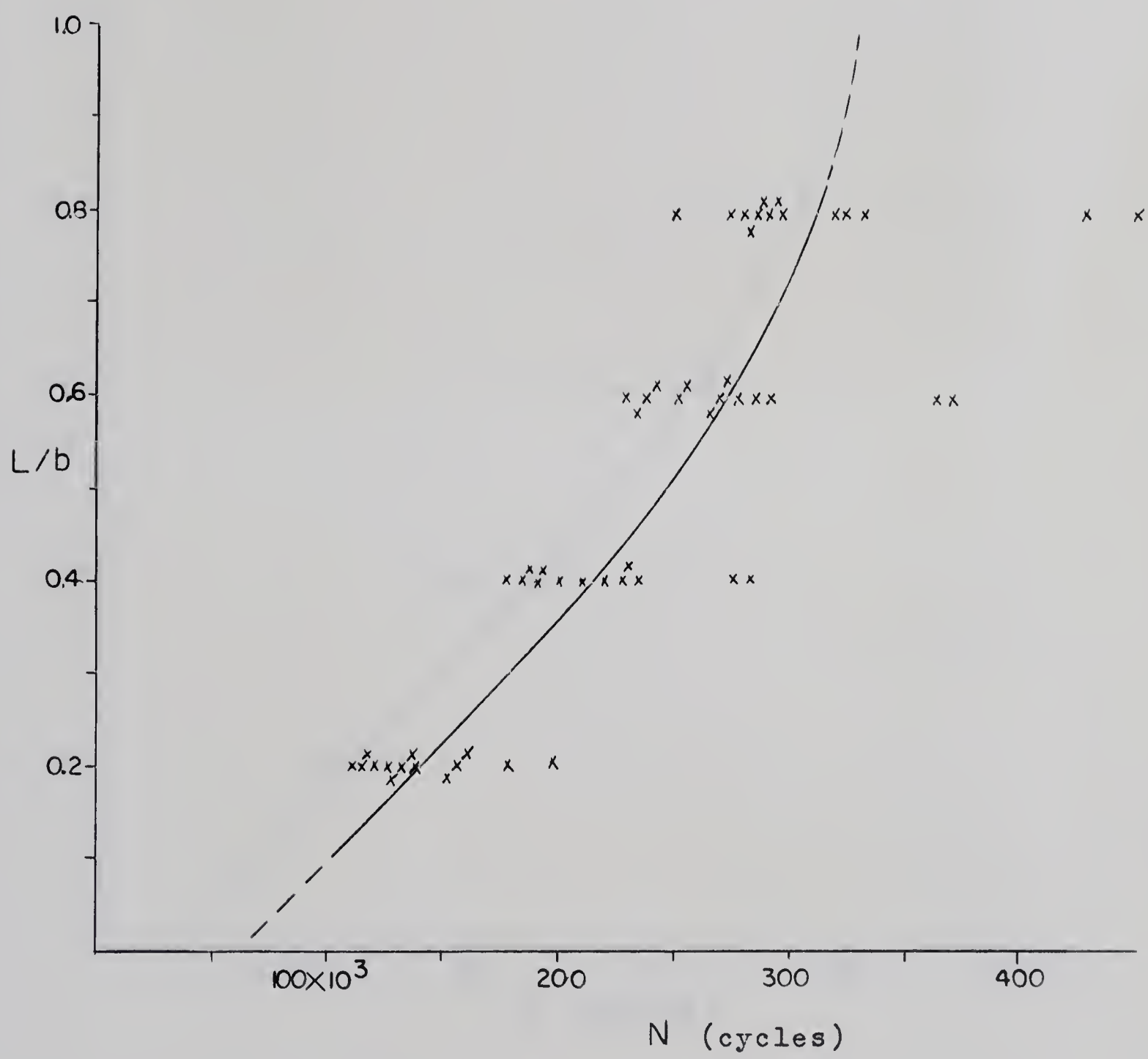

Figure 4.2 Crack Growth for Tests with Range of Stress of ±21 ksi, Mean Stress of Zero.

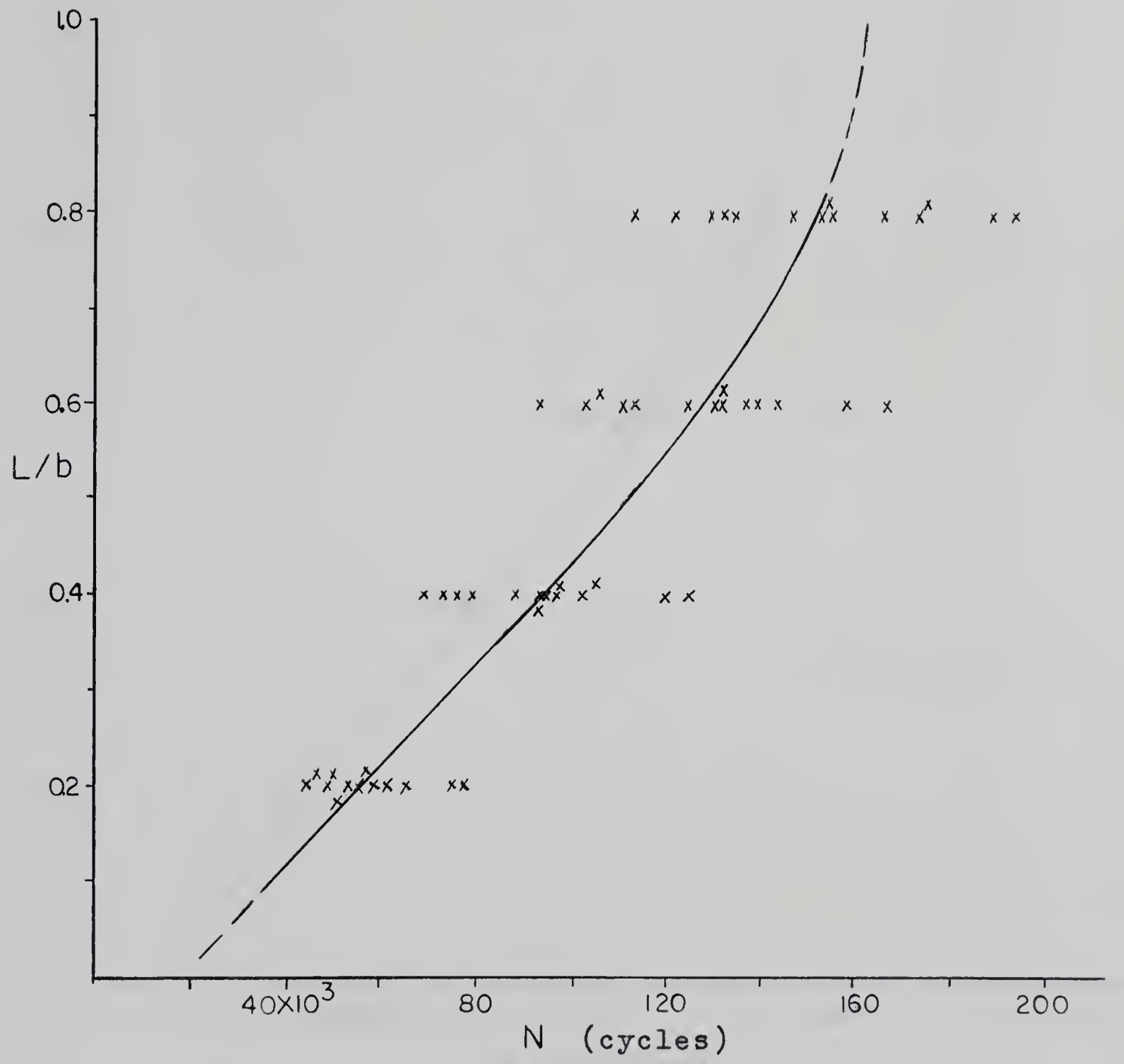

Figure 4.3 Crack Growth for Tests with Range of Stress of $\pm$ 26 ksi, Mean Stress of Zero

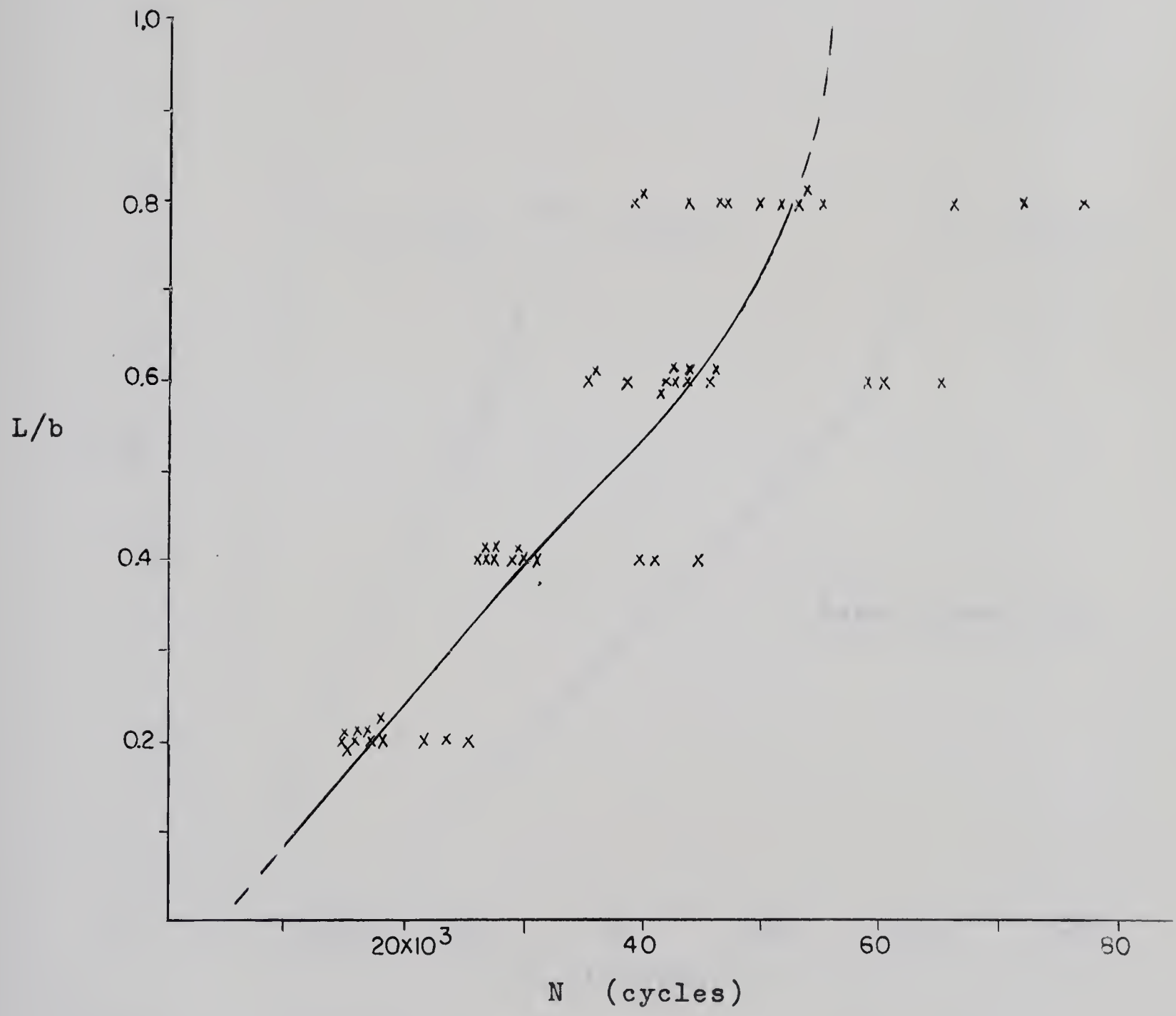

Figure 4.4 Crack Growth for Tests with Range of Stress of $\pm$ 35 ksi, Mean Stress of Zero

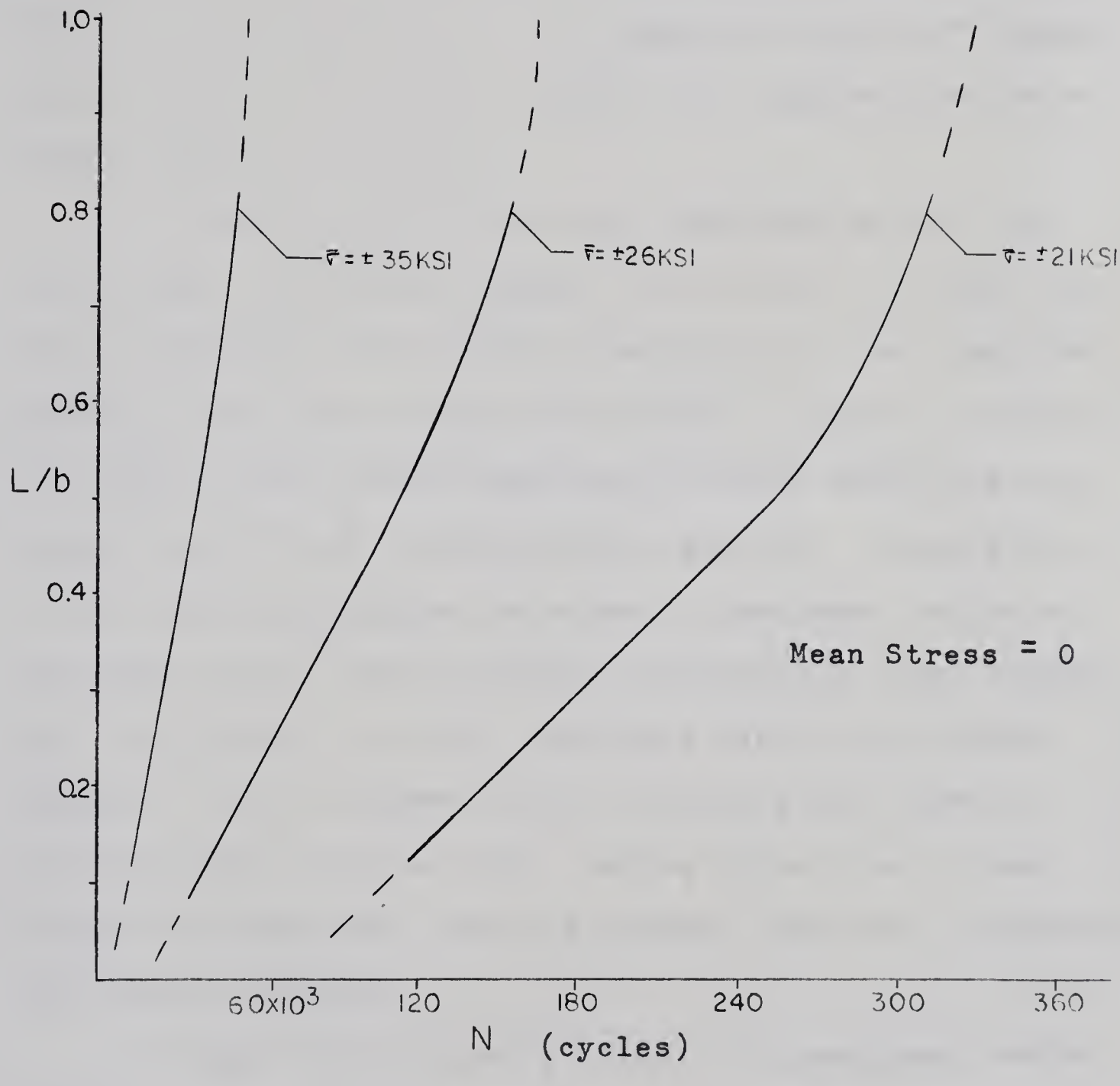

Figure 4.5 Average Curves from Series A Tests

since the number of cycles to initiation was not known exactly.

Individual tests are shown in Figures 4.6, 4.7 and 4.8. In Figures 4.6 and 4.7 each curve represents the average of the two cracks which develop from the two notches in each specimen. The graph in Figure 4.8 represents growth of individual cracks in a typical test at a stress range of $\pm$ 35 ksi.

In nearly all of the tests conducted at the two lower ranges of stress, namely $\pm$ 21 ksi and $\pm$ 26 ksi, the rate of extension was nearly constant until the crack had propagated half way across the section. However, tests at the higher stress level characteristically exhibited the type of curve shown in Figures 4.4 and 4.8. Observation of the crack propagation patterns of specimens tested at this high stress level revealed considerable crack branching. In contrast to this, specimens tested at a stress range of $\pm$ 26 ksi showed little branching and those at $\pm$ 21 ksi almost none at all. Having noted this it was decided to completely fracture several specimens to examine the fracture surface.

It was found in nearly all of the specimens tested at $\pm$ 35 ksi that initial fracture occurred on a surface normal to the surface of the specimen, but gradually part of the fracture surface became inclined at a decreasing angle to the surface of the specimen. In all cases this

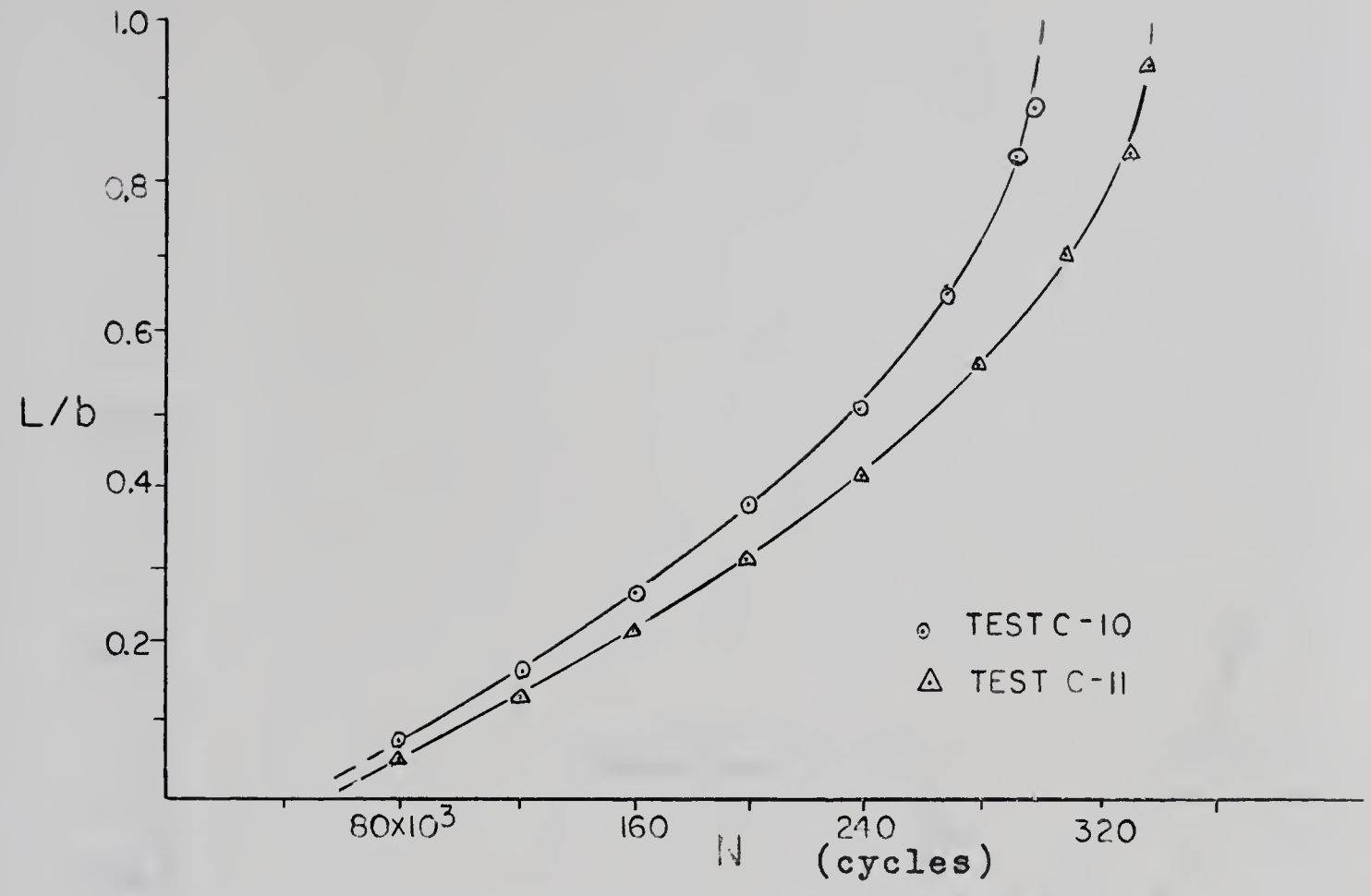

Figure 4.6 Typical Individual Tests at $\pm$ 21 ksi

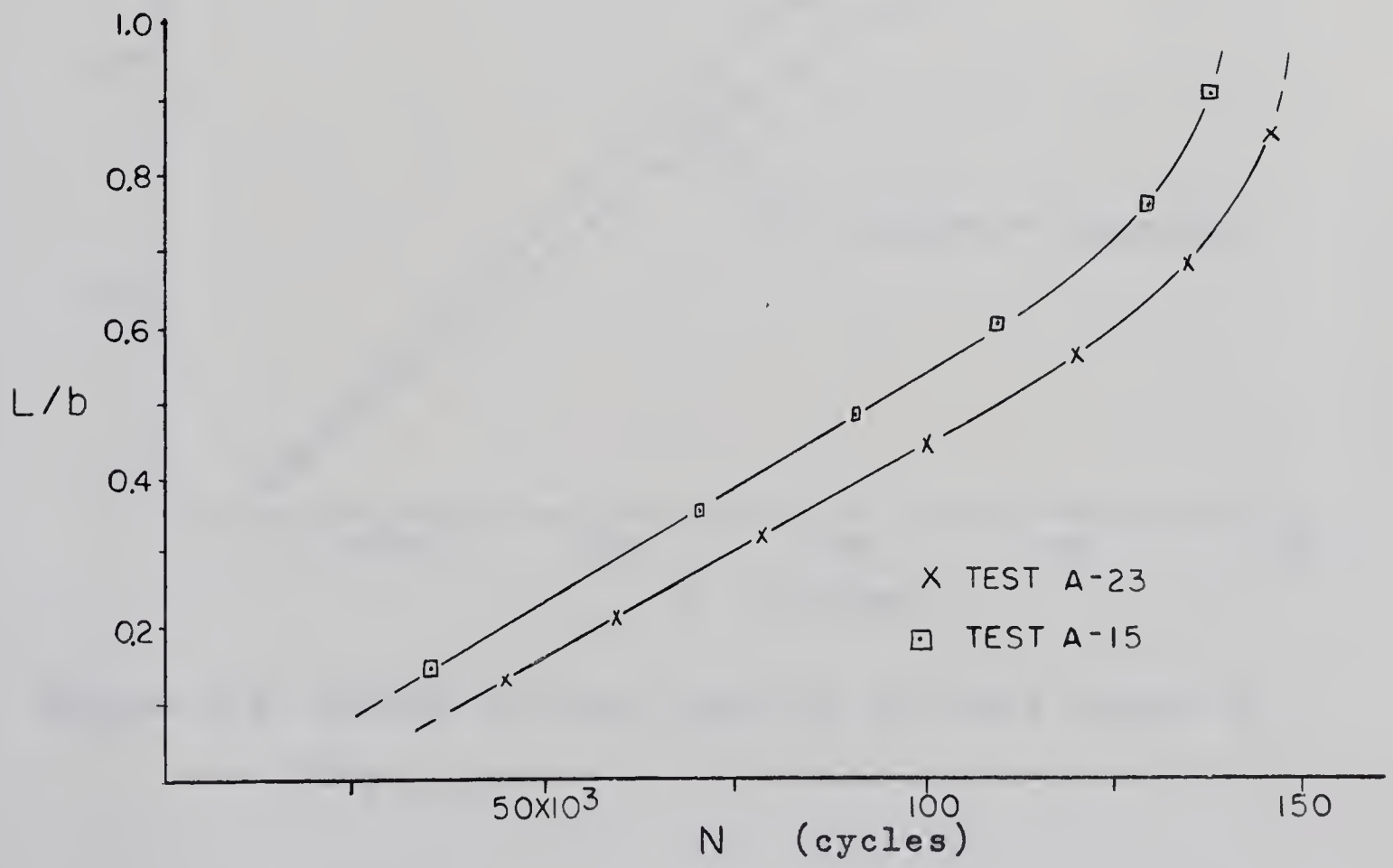

Figure 4.7 Result of Typical Tests at $\pm$ 26 ksi

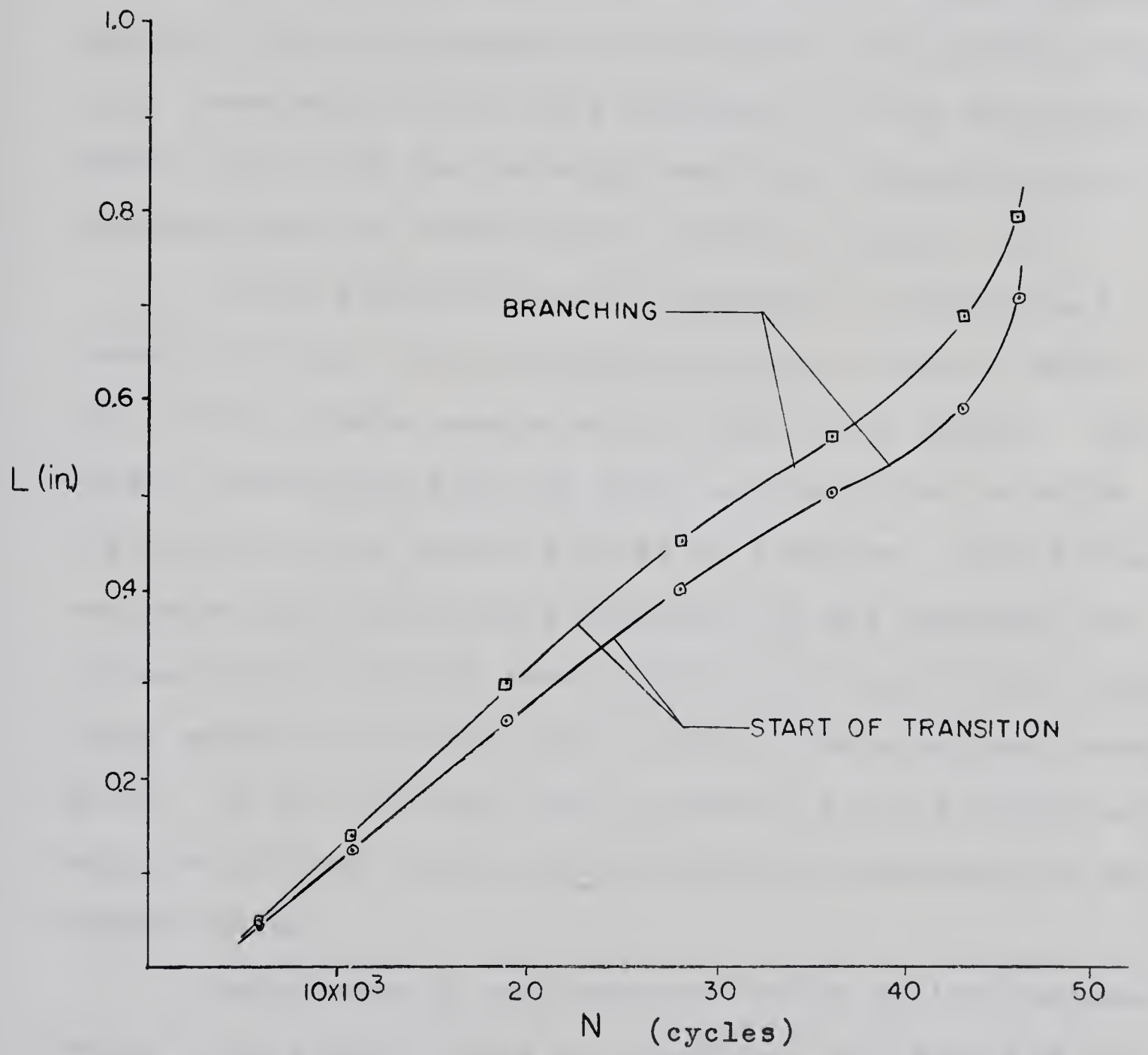

Figure 4.8 Growth of Each Crack in Specimen Tested at ± 35 ksi

transition of the fracture surface occurred either above or below the neutral axis. On the side opposite to that on which this transition occurred the crack proceeded in the expected direction. This decreasing inclination of the fracture plane caused the surface crack to deviate from the expected line of propagation as shown in the sketch in Figure 4.9. Eventually a new crack branched out from some point behind the tip of the existing crack and propagated at an increased rate as shown by the curves in Figure 4.8.

In the particular case represented in Figure 4.8 rotation of the fracture surface became noticeable after each of the cracks reached about 0.35 in. in length. This length corresponds with the point on the curves at which the rate of crack growth started to decrease. This decrease continued until new cracks branched out and extended past the existing cracks at about 0.55 in. for each of the cracks. These points correlated well in all of the specimens investigated. Of the fourteen tests conducted at this stress level, only two did not display this transition phenomenon to any marked extent.

Photographs of the fracture surface of the specimen whose crack growth curves are presented in Figure 4.8 are presented in Figures 4.10 and 4.11.

Fracture surfaces of the specimens tested at a stress range of $\pm$ 26 ksi exhibited the same characteristics as the above but with less severity. In these tests the cracks did

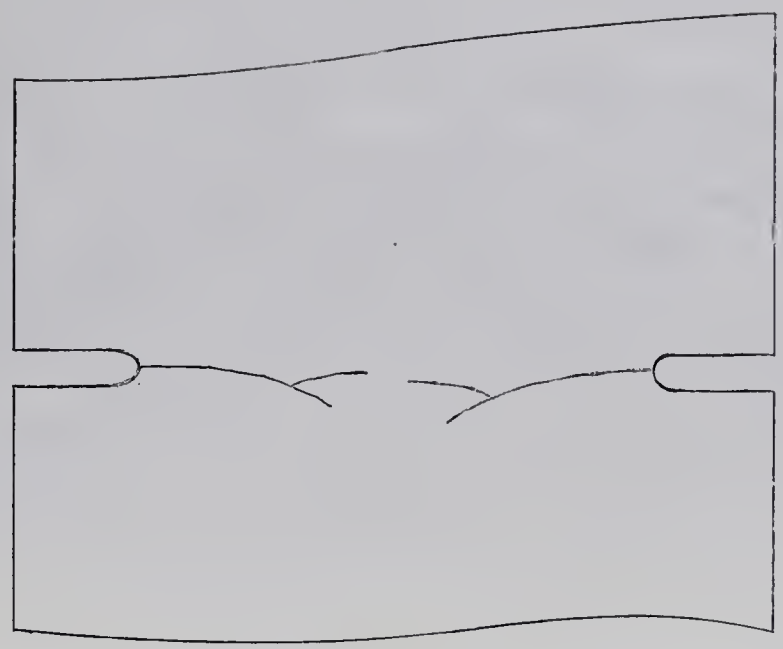

Figure 4.9 Crack Propagation Pattern in Tests at ± 35 ksi

not rotate through the large angle noted in the previous test set. In tests at the lowest stress level the transition phenomenon was not noticeable.

4.2 Results of Series B

Series B tests were conducted to determine the effect of mean stress and range of stress on the rate of fatigue crack propagation. The first set of tests was conducted at an initial nominal stress range of ± 21 ksi and zero mean stress, the results of which are shown in Figure 4.12. Figures 4.13 and 4.14 represent tests in which the range of stress was the same, but mean stresses of 3 ksi and 6 ksi

Figure 4.10 View of Fracture Surface

Figure 4.11 Close-up View of Fracture Surface

respectively were applied. The final test set of this series, shown in Figure 4.15, was conducted at a zero mean stress with a range of stress of $\pm$ 24 ksi. In all of these graphs the curves shown are arithmetic mean values and the points represent results from individual tests. The average curves presented in Figures 4.10 to 4.13 are combined in Figure 4.16 to illustrate the comparison between the various tests.

The transition of the fracture surface which was mentioned in Section 4.1 was not noticeable in the tests represented by Figure 4.12, but some crack branching was noted. In the set of tests conducted with a mean stress of 3 ksi and a stress range of $\pm$ 21 ksi some transition of the fracture surface occurred, becoming noticeable for values of L/b greater than 0.4. The angle of inclination of the fracture surface to the surface of the specimen, which was initially ninety degrees, was not noted to decrease by more than about ten degrees. In the tests represented by Figure 4.14 the transition phenomenon was found with varying severity. The transition became noticeable at a value of L/b of 0.3 in one test and the fracture surface rotated through about fifteen degrees before crack branching occurred, but in other tests the transition was less noticeable. In the set conducted with zero mean stress and a stress range of $\pm$ 24 ksi some of the tests showed appreciably no rotation of the fracture surface, while other tests showed a slight transition for L/b greater than 0.6.

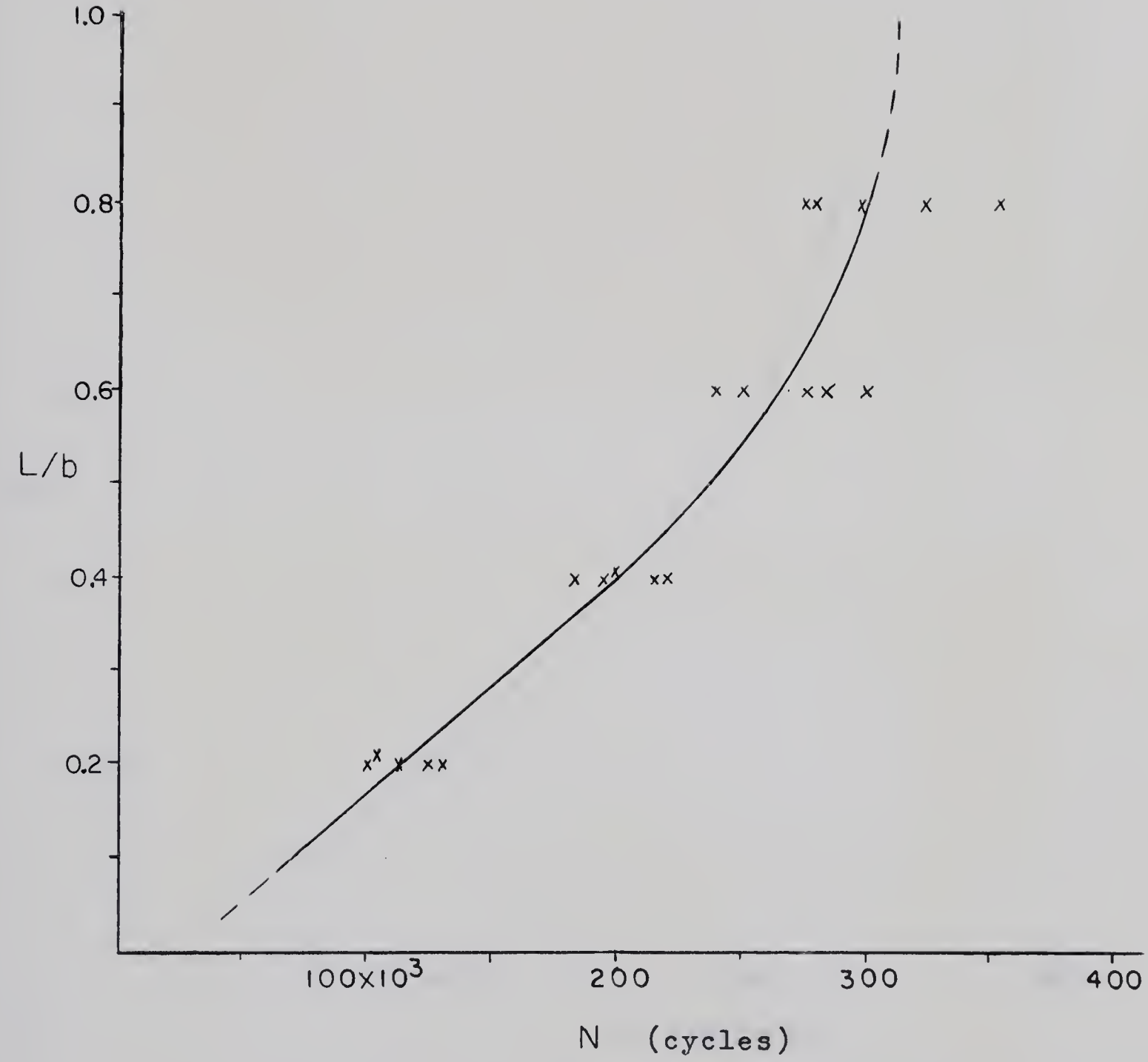

Figure 4.12 Crack Growth for Tests with Range of Stress of $\pm$ 21 ksi, Mean Stress of Zero

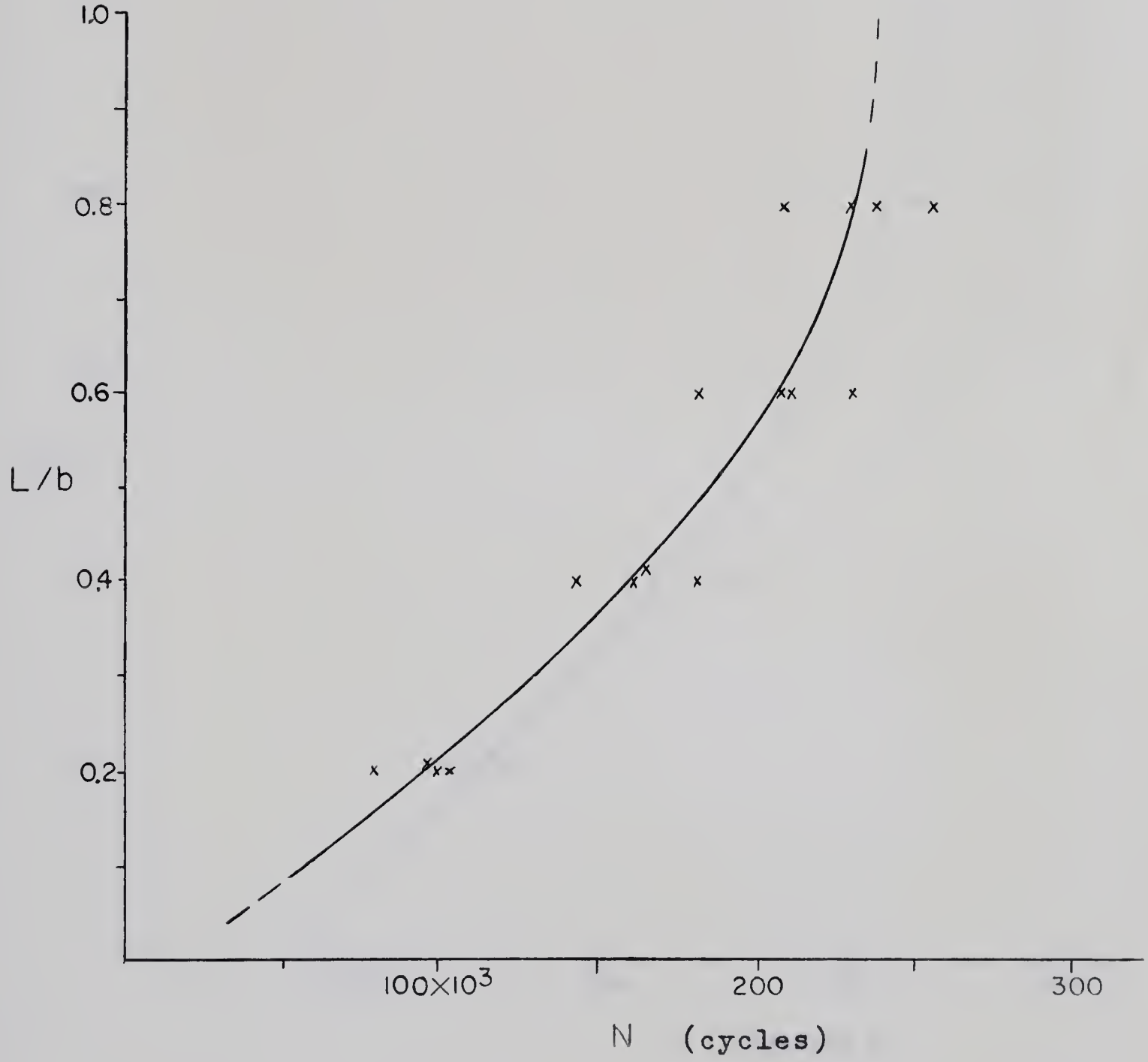

Figure 4.13 Crack Growth for Tests with Range of Stress of $\pm$ 21 ksi, Mean Stress of 3 ksi

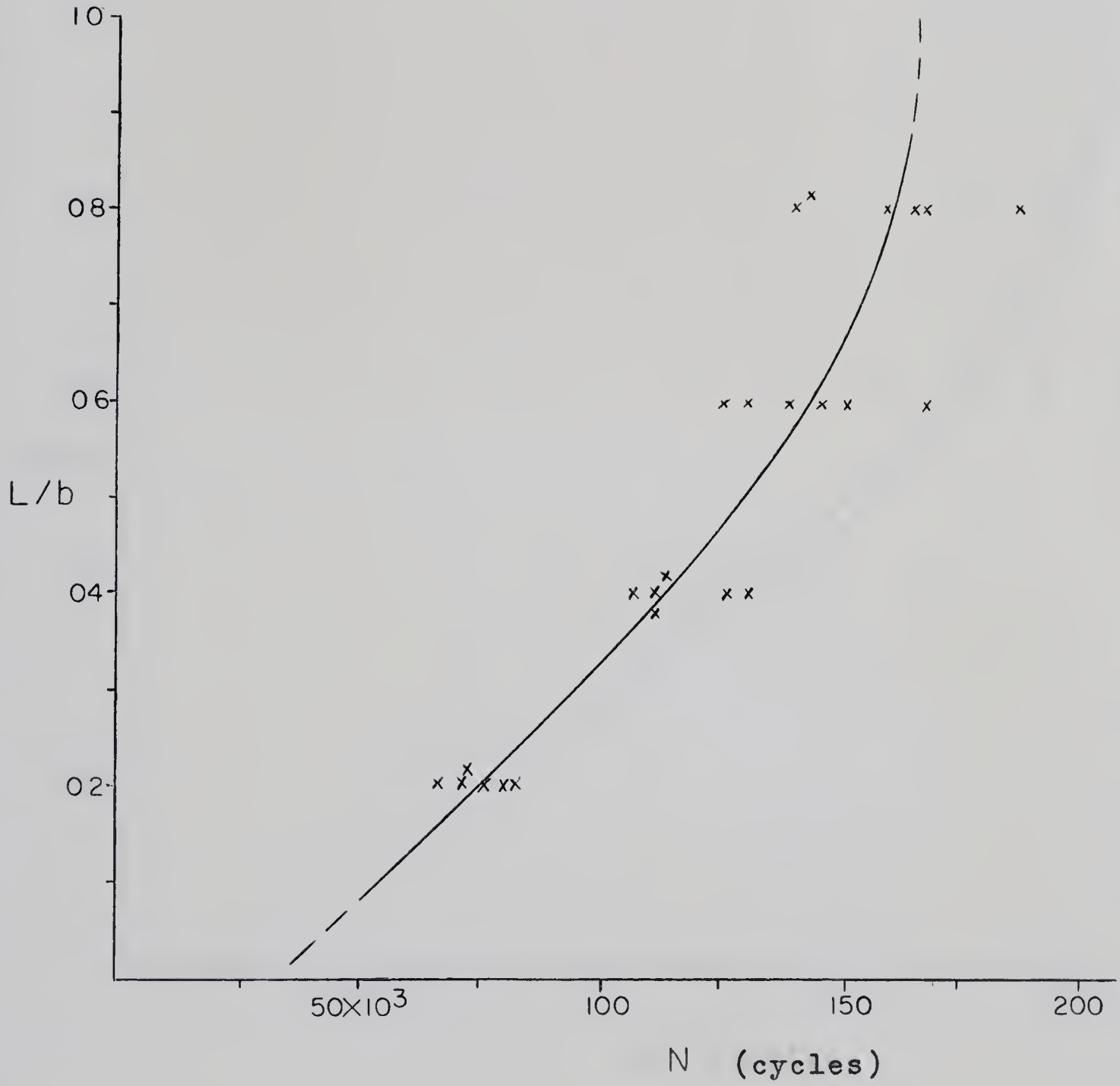

Figure 4.14 Crack Growth for Tests with Range of Stress of ± 21 ksi, Mean Stress of 6 ksi

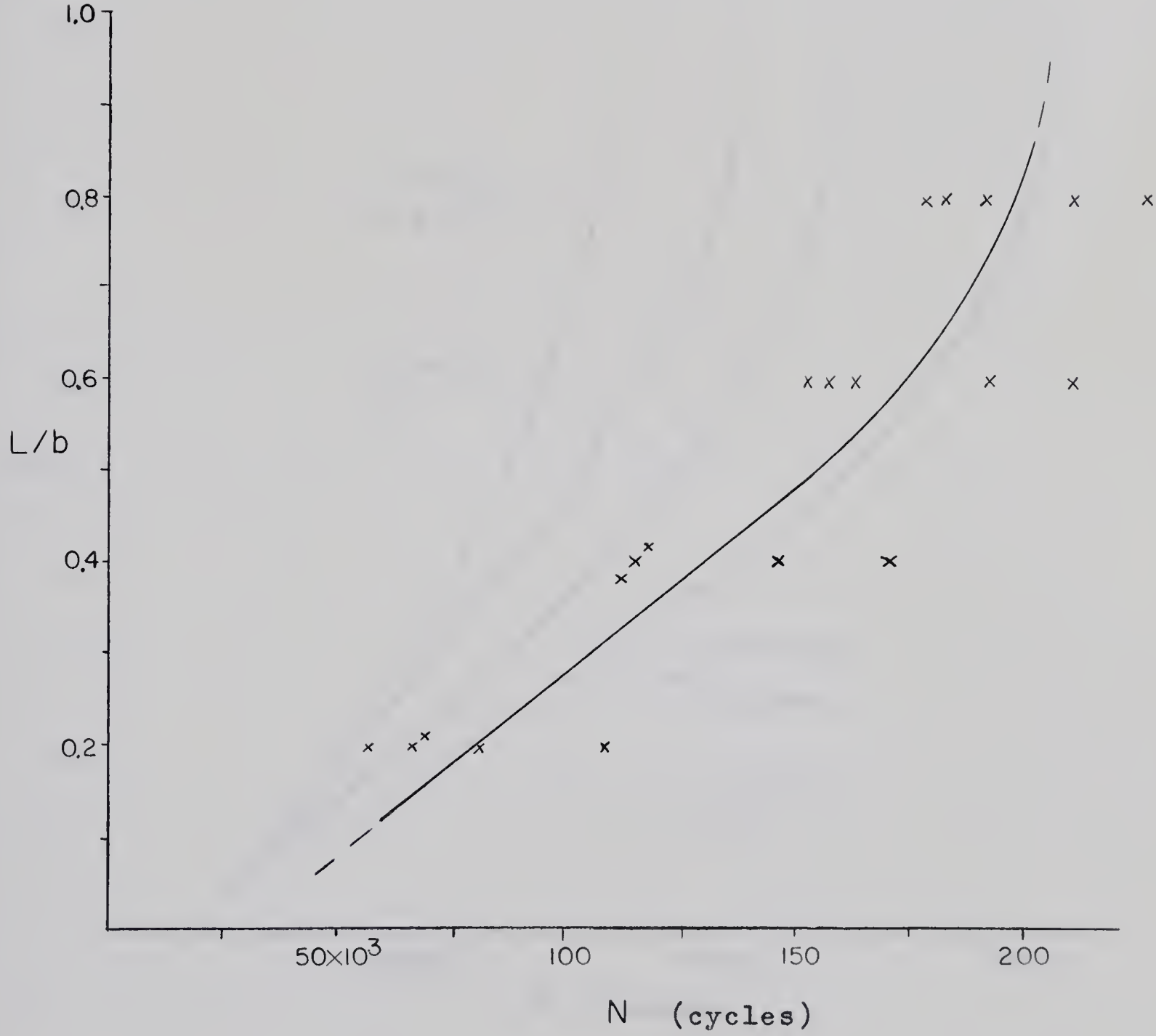

Figure 4.15 Crack Growth for Tests with Range of Stress of ± 24 ksi, Mean Stress of Zero

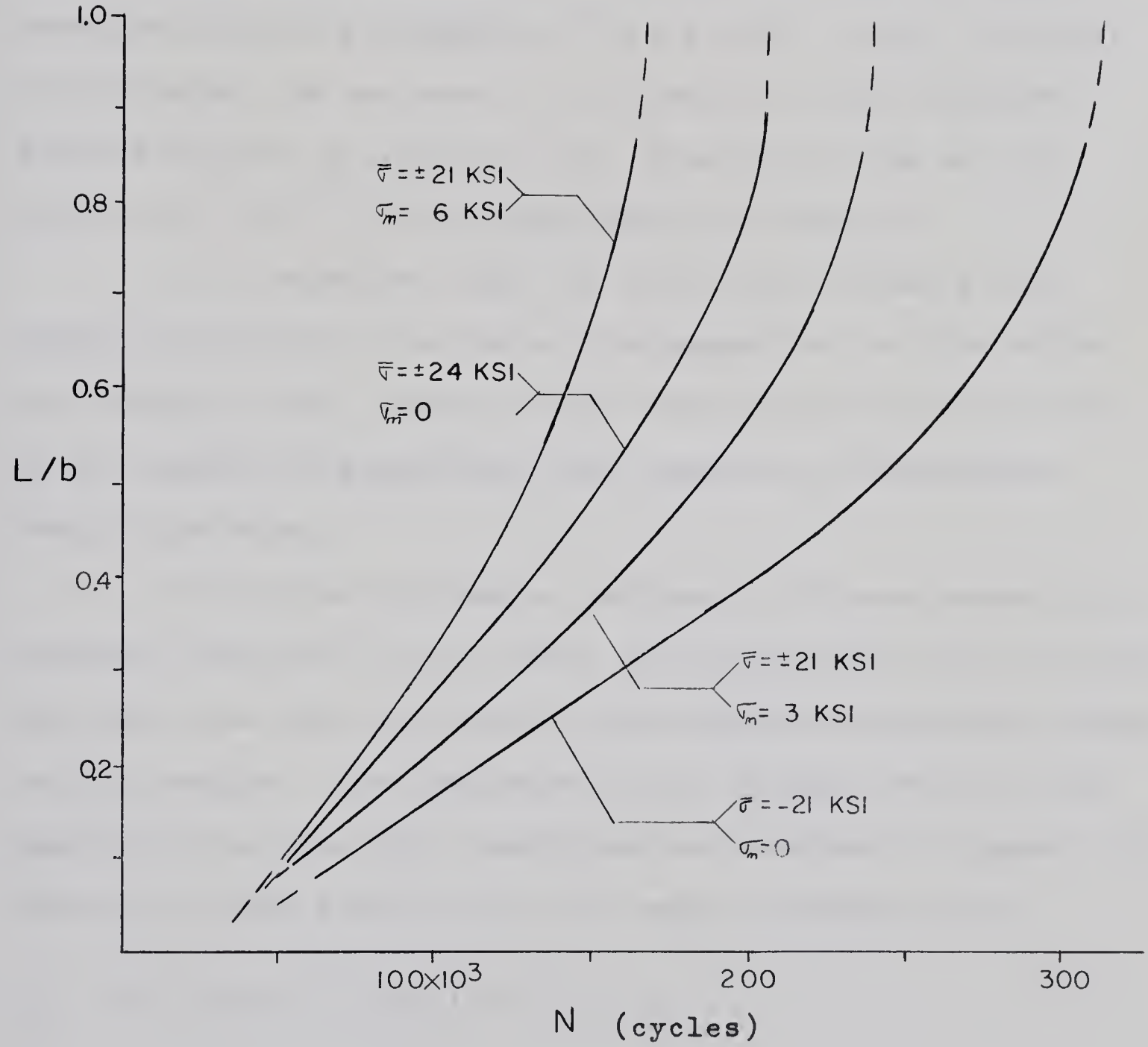

Figure 4.16 Average Curves from Series B Tests

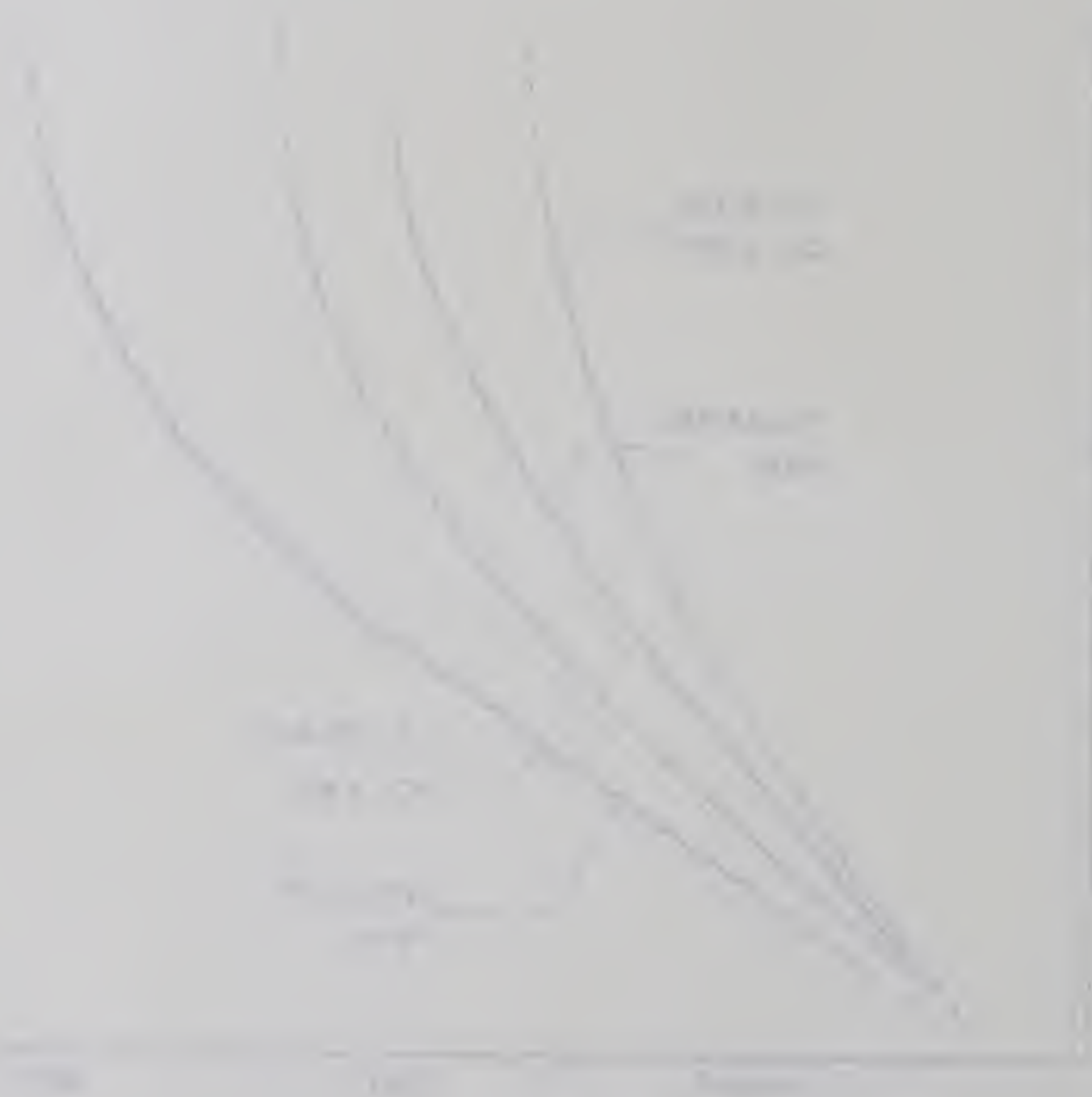

As found in Series A, when transition of the fracture surface occurred, it occurred on only one side of the neutral axis.

In none of the tests in Series B did this transition and branching cause the fluctuation in the rate of crack propagation such as appear in Figure 4.8. In the fractures investigated the decrease of inclination of the fracture surface was not as large as that observed in the set of tests with the $\pm$ 35 ksi stress range in Series A.

It is expected that the transition actually did cause variations in the rate of propagation, but the effect was probably small enough in the cases presented here that it was masked by measuring crack length at sufficiently large intervals.

The curves in Figures 4.12 and 4.15 have essentially straight portions up to a value of L/b of about 0.40, whereas the other two sets of results show slightly increasing slopes in this region. The influence of the fatigue crack on the applied stress for this configuration is shown in Figure 4.17. There is little effect up to L/b equal to about 0.40.

4.3 Discussion of Results-Series A

The rates of crack propagation for various points on the average curves presented in Figures 4.2 to 4.4 and Figures 4.12 to 4.15 are shown in Table I. The values in the second column were determined from the straight portion of the curves

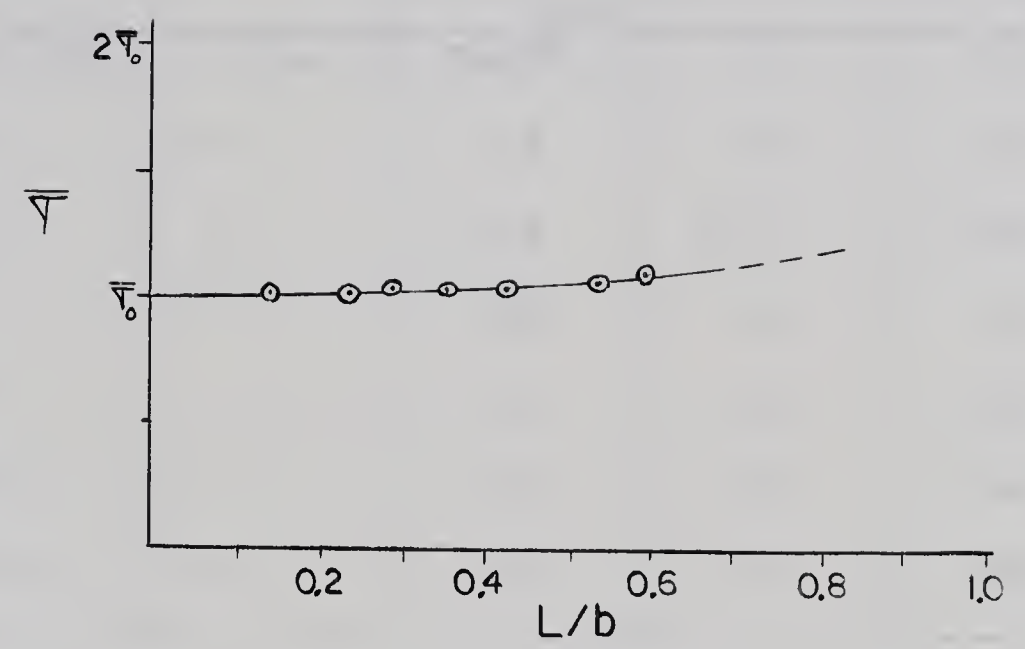

Figure 4.17 Effect of Crack on Applied Stress Range

where applicable; otherwise these values are averages up to L/b equal to 0.40. Quantities in the third and fourth columns were determined from tangents to the curves at values of L/b of 0.6 and 0.8. In the case of the test with the stress range of $\pm$ 35 ksi the rates of propagation were determined from two tests which displayed a minimum of the shear transition phenomenon mentioned previously, since there is little point in comparing tests in which the modes of failure apparently differ. Table I is divided into two parts to separate tests conducted in Series A from those in Series B. A plot of the rates of crack propagation for Series A tests versus ranges of stress on a log-log graph (Figure 4.18) indicates a linear relationship between the quantities, with a slope of four, on the

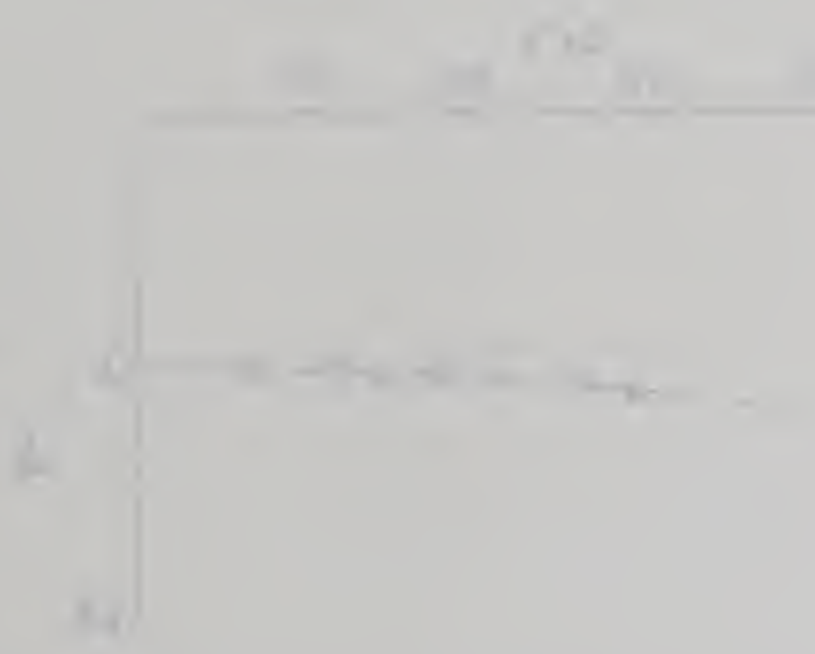

TABLE I

Range of Stress	Mean Stress	dL/dN (in./cycle)			Number of tests
		L/b up to 0.40	L/b=0.60	L/b=0.80	
± 21 ksi	0 ksi	2.7×10^{-6}	4.0	6.7	14
± 26	0	5.3	6.9	11.6	14
± 35	0	17.4	25.0	58.0	2
± 21	0	2.4	3.9	8.5	5
± 21	3	3.1	5.4	11.5	4
± 21	6	5.4	8.2	16.4	6
± 24	0	4.1	6.2	12.0	5

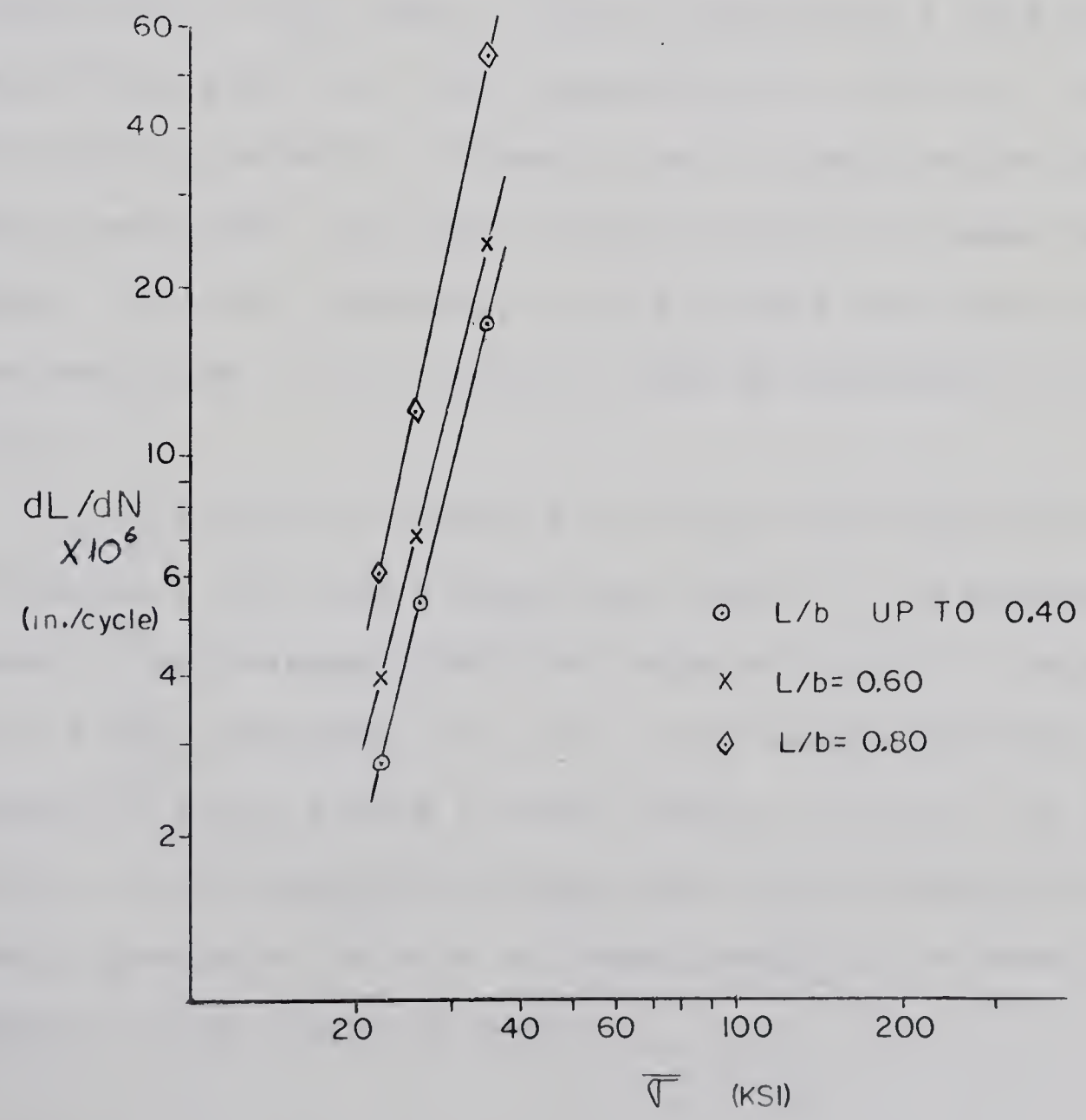

Figure 4.18 Rate of Crack Propagation Versus Applied Stress Range Based on Data from Series A Tests

basis of a curve through three points. Actually, this set of results could be presented on a single straight line if the applied stress as a function of crack length were accurately known.

4.3.1 Comparison with Head theory

While measuring crack lengths during the testing program it was noted that the size of the plastic zone at the crack tip appeared to increase as the crack extended. This was observed visually since distortions caused by plastic deformations apparently changed the reflective properties of this zone. Where viewed with a five power magnifying glass the zone appeared quite distinct from surrounding material. However, as no quantitative measurements were made, the exact nature of this increase was not known. If this observation was accurate then this is a contradiction of the theory of Head as discussed in Section 2.2.1.

In Figure 4.19 data from Figure 4.3 was used to plot $L^{-1/2}$ versus N for this average test result. In plotting this graph it was assumed that the crack extended to the edge of the test specimen (i.e. the crack length includes the length of slot) giving a crack length of 0.5 in. at 36,000 cycles. An assumption of this type is necessary since Head's theory predicts the rate of crack growth to be zero if the present crack length is zero.

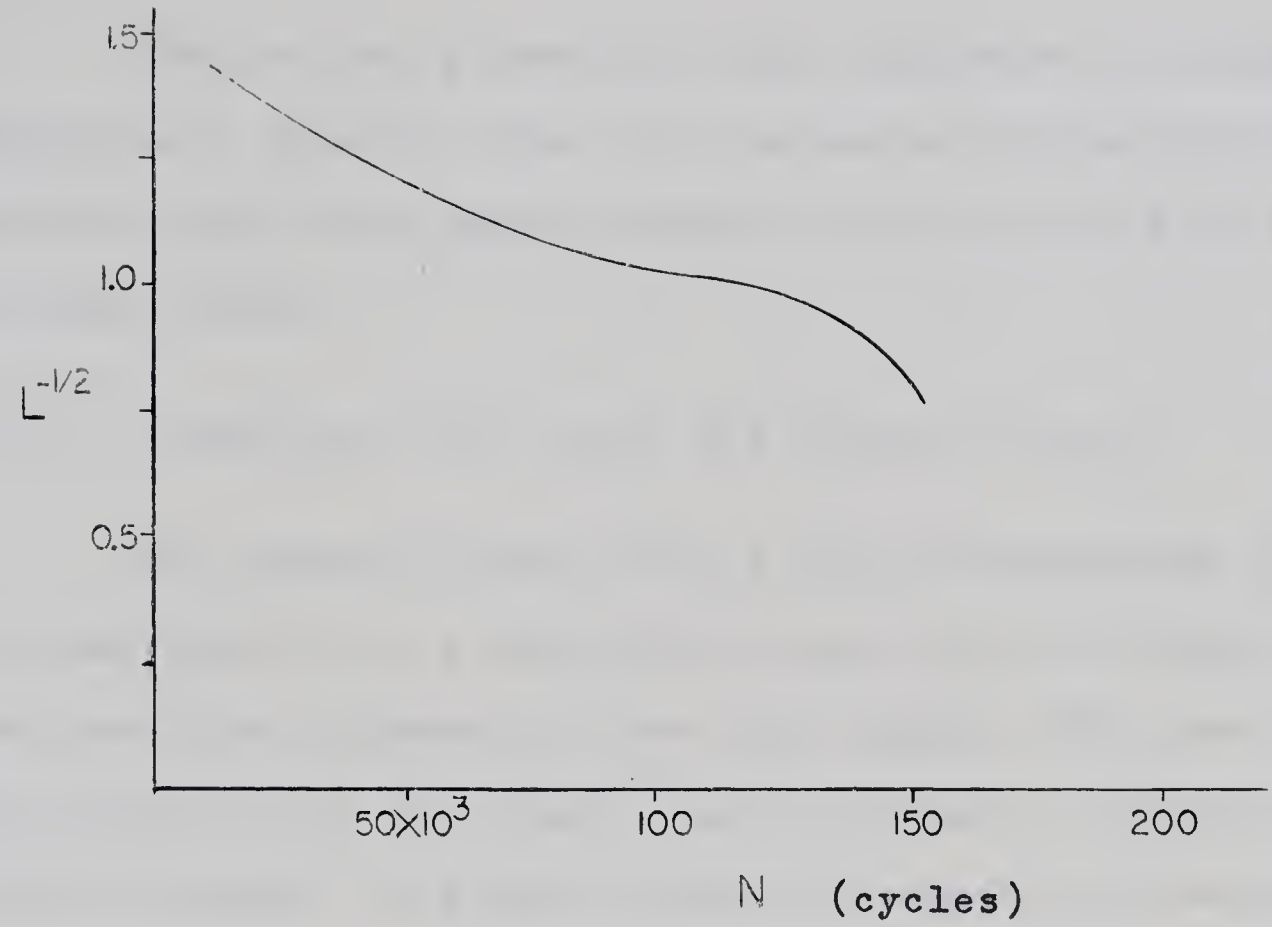

Figure 4.19 Figure 4.3 Replotted According to Head Theory

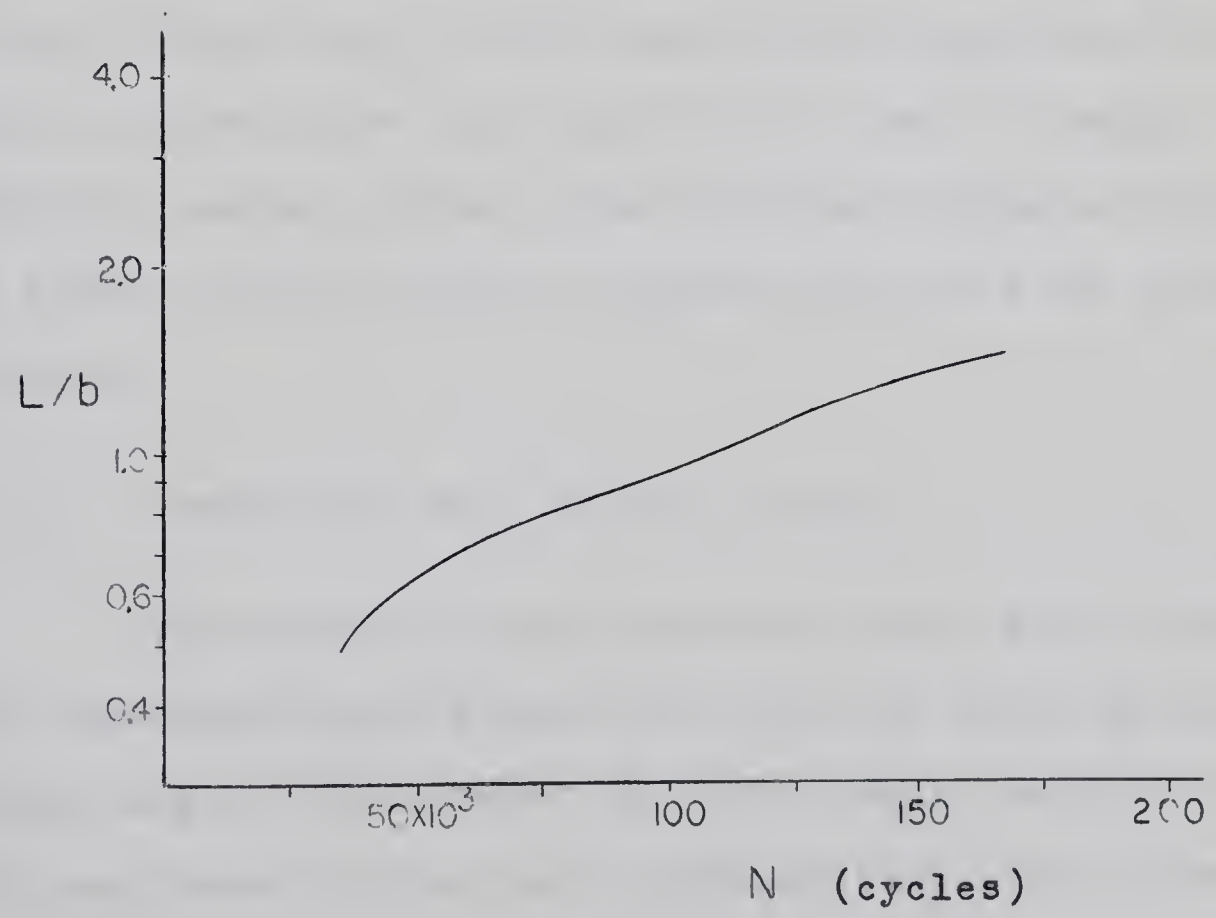

Figure 4.20 Data from Figure 4.3 Plotted on Semi-Log Basis

Head's theory predicts that the graph in Figure 4.19 should be a straight line for the period during which constant stress cycles were applied which in this case is up to about 105,000 cycles.

4.3.2 Comparison with Frost and Dugdale Theory

The average result of the tests represented by Figure 4.3 was plotted on a semi-logarithmic scale in Figure 4.20. The theories proposed by Frost and Dugdale (10) and Liu (11, 12) predict that the crack length increases exponentially with the number of stress cycles for constant stress range and mean stress. These theories also predict a zero rate of crack growth when the crack length is zero, so that it is necessary to make an assumption concerning an initial crack length such as that made in the previous section (i.e. it is assumed that the crack is 0.5 in. in length after 36,000 loading cycles). The Frost and Dugdale theory predicts a linear relationship in Figure 4.20 for N up to about 105,000 cycles.

4.3.3 Comparison with Weibull Theory

The Weibull theory predicts that, for a fixed range of stress and mean stress, the rate of crack growth is constant and not influenced by the current length of crack. It was found for the test configuration used in Series A that the nominal stress amplitude was constant for values

of L/b up to 0.5. For the tests conducted with stress ranges of $\pm$ 21 ksi and $\pm$ 26 ksi (both with zero mean stress) the rate of crack propagation over the corresponding period was found to be constant (In some cases a small increase in growth rate was noted over this period). This was not found to be true for the tests with a stress range of $\pm$ 35 ksi (and zero mean stress) but in these tests a transition of the fracture surface occurred (See Section 4.1). This transition apparently influenced the rate of crack growth.

4.4 Discussion of Results-Series B

A study of the results presented in Figure 4.16 indicates that the value of the mean stress does influence the rate of crack propagation.

In three of the test sets the range of stress was equal, but varying values of mean stress were applied. The results indicate an increasing rate of crack growth for an increasing mean stress. Extrapolation of the curves back to $L/b = 0$ indicates that the mean stress may not have influenced the number of cycles to initiation. On the other hand, two of the test sets initially had the same peak stress of $\pm$ 24 ksi. However, the rate of crack propagation for the set with a mean stress of zero was higher throughout most of the life of the specimen, even though the other set actually had an increasing peak stress. This indicates that the range of stress may be a more important factor in determining the rate of crack growth than is the mean stress.

The test results indicate that the dependence of the rate of crack growth on the applied stress may be represented by a factor $\frac{\bar{\nabla}^n}{N_s}$, where $\bar{\nabla}$ is the applied stress range, N_s is a constant for a given range of stress, and n is a material constant. This type of dependence has also been suggested by Frost and Dugdale (9), Liu (12,15) and Weibull (18).

In Series B of the investigation, in which the specimens were tested in a fixed-end configuration, it was found that the bending moment at the test section was constant as long as the combined crack length was less than about 40 per cent of the specimen width. Over this range tests conducted with a zero mean stress (Figures 4.12 and 4.15) had a constant rate of crack extension. For the tests in which the mean stress was not zero the rate of crack extension increased slightly over this range, but this can be attributed to the fact that there was an increasing mean stress, i.e. an increasing peak stress, since the total axial load on the specimen was constant.

4.5 Further Observations

1. It was previously mentioned that it is thought that a fatigue crack grows in a series of steps rather than in a continuous manner (Section 2.1). In one of the tests conducted using the fixed-end configuration with a range of stress of $\pm$ 24 ksi, increases in crack length of the order of 0.010 in. were measured in 500 cycles of loading.

It was believed that this indicated that the process could be regarded as continuous for the purpose of presentation of results, since in this case the specimen life was about 200,000 cycles.

2. At no time during the testing program did the situation arise where a crack did not propagate from a notch but occasionally it was observed that more than one crack formed at a notch, only one of which propagated. This lack of non-propagating cracks was likely due to the rather high stress levels involved. As previously mentioned, a considerable amount of crack branching was observed, occurring more often at high stress levels, but formation of a new crack ahead of an existing crack was rarely observed, except occasionally near the end of the specimen life.

3. It seems reasonable that the rate of crack propagation is defined by the actual stress existing in the region of the crack tip. Then, considering a test specimen subjected to a constant nominal stress based on the remaining area, the rate of crack propagation will be constant if the stress concentration factor is constant. On the other hand, if this factor increases in proportion to the crack length, then the crack length can be expected to increase exponentially with the number of applied stress cycles. Evidently, however, the above conclusion means that there are any number of other possibilities; e.g. the stress concentration factor could increase in proportion to some power of the

crack length. The present investigation appears to support the constant stress concentration factor.

4. It was mentioned in Section 1.5 that fatigue cracks generally propagate in a trans-granular manner. Metallurgical specimens containing fatigue cracks from test specimens were prepared to find whether this occurred in the low-carbon mild steel tested. Microscopic inspection revealed that the propagation was mainly inter-granular (See Figure 4.21), although a few exceptions were noted. It is speculated that this was due to the existence of iron carbide on the grain boundaries which caused the boundaries to be more vulnerable to fatigue damage than the grains.

5. In Section 2.3 it was stated that the crack length was expected to decrease from the specimen surface toward the neutral axis. Inspection of fatigued specimens which contained dye-penetrant stains confirmed this suggestion.

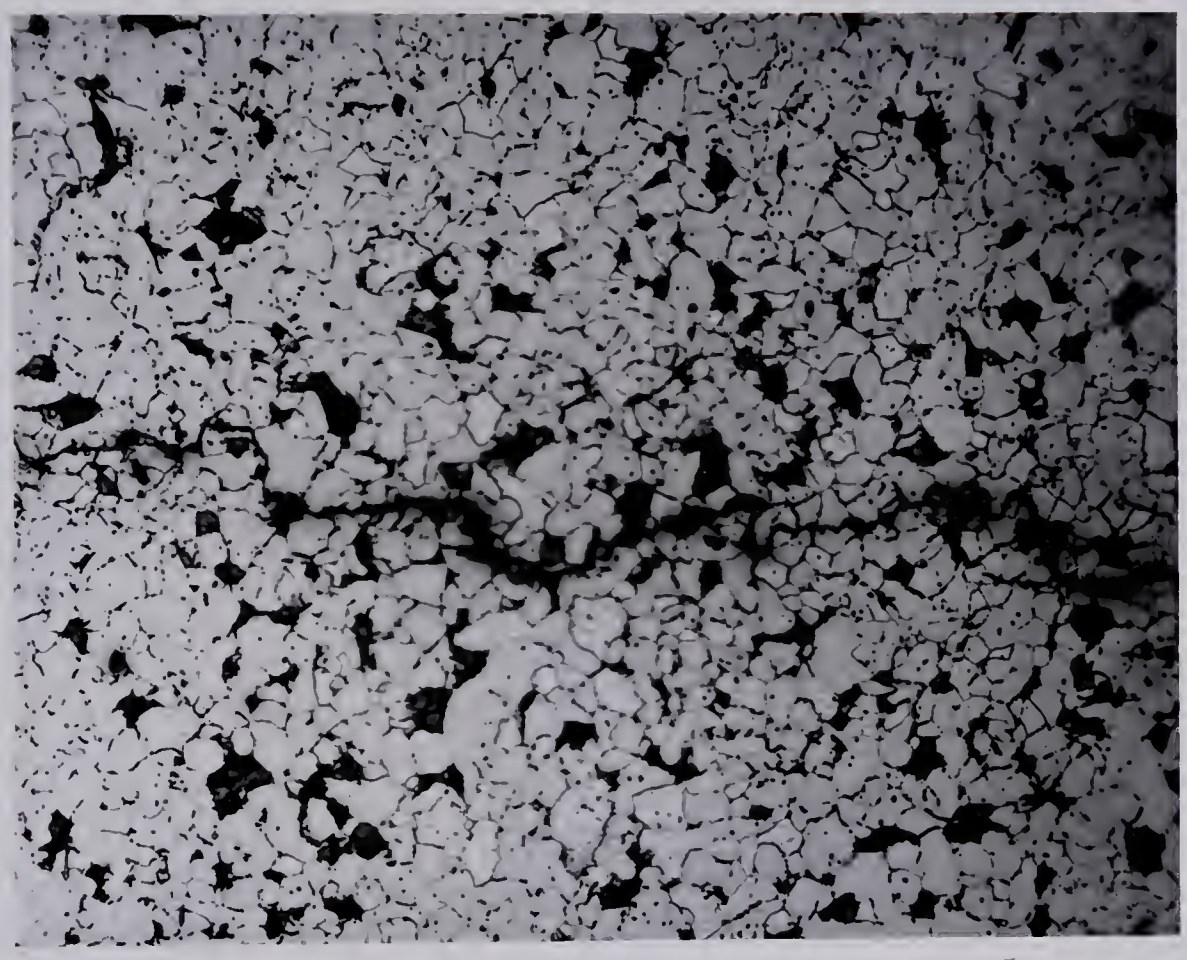

Figure 4.21 Photograph Showing Intergranular Nature of Crack Propagation (x70)

CHAPTER V

CONCLUSIONS AND RECOMMENDATIONS

5.1 Conclusions

In a recent publication, Paris and Erdogan (18) pointed out the dangers involved in drawing conclusions from a limited amount of data on fatigue crack propagation. They showed that some arbitrarily selected measurements of fatigue crack growth apparently confirmed different theories of crack propagation. Heeding this warning, the following conclusions were reached.

The tests conducted in Series A of the investigation indicated that the rate of crack extension was proportional to the fourth power of the nominal stress range, although this is based on very limited data. From tests of axially loaded mild steel specimens Frost and Dugdale (10) suggested this index should be three, while Paris and Erdogan (13,18) suggested a value of four for aluminum.

Test Series B showed that the rate of crack growth was affected by the value of the mean stress for the particular type of tests conducted. Frost and Dugdale (10) found that the mean stress did not affect the crack extension in mild steel, but did in aluminum. It does not seem possible that the value of the mean stress could have no affect on the rate of crack growth for all values of mean stress, as discussed in Section 2.5. The Series B tests also suggested that

the range of stress may be more important in determining the rate of crack growth than the mean stress. No quantitative conclusions could be reached since the mean stress was not constant in the tests.

Results of the present investigation appear to agree with the Weibull theory of crack propagation insofar as this theory predicts a constant rate of crack growth under a constant nominal stress range and mean stress. The results suggest that, for the problem investigated, the rate of crack growth is given by

$$\frac{dL}{dN} = \frac{\bar{\nabla}^n}{N_s}$$

where $n = 4$ and, determined from tests in Series A with zero mean stress, $N_s = 0.086$ kips^4-cycles/in.^{9}

Due to insufficient data, no definite conclusions could be reached regarding the transition of the fracture surface which was discussed in Chapter IV. It is believed that the phenomenon was caused by transverse shearing stresses which changed the directions of the principal stresses. These shearing stresses could have been due to the nature of the loading or could have been caused by constraint of plastic deformation set up by fibres adjacent to the plastic zone. It appeared that the transition and branching increased in severity with increases in the maximum stress.

5.2 Summary of Conclusions

1. Results of the tests conducted were in agreement with the Weibull theory of crack propagation; for constant stress range and mean stress the rate of crack growth was constant.

2. For these tests it appeared that the rate of crack growth was proportional to the fourth power of the range of applied stress.

3. Test Series B revealed that the value of the mean stress did influence the rate of crack extension but indicated that the range of stress was more influential in determining this rate than was the mean stress.

4. The gradual rotation of the fracture surface which was noted in tests at the higher levels of stress was apparently caused by a transverse shear stress.

5. For the tests conducted it was found that the rate of crack propagation could be predicted by

$$\frac{dL}{dN} = \frac{\bar{\nabla}^n}{N_s} \quad .$$

In this expression, $\bar{\nabla}$ is the stress range, n is a material constant, and N_s is a constant depending on the mean stress.

5.3 Recommendations

It is desirable that more of the Series A tests be conducted at stress levels different from those in this investigation. Each curve in Figure 4.18 was drawn through

only three points and, although this indicated that the rate of crack growth depended on the fourth power of the stress range, it was not conclusive.

Testing of wider specimens under the same conditions would indicate whether the rate of crack propagation is dependent on specimen width, as proposed by Weibull (16). These tests would also serve as a further check on the propagation theory.

The test Series B was not satisfactory to quantitatively study the effect of mean stress on the rate of crack growth due to the increasing mean stress. A test should be devised in which both mean stress and stress range can be held constant in order to study this effect.

5.4 Practical Applications

Results presented in Chapter IV indicate that a fatigue crack can be initiated quite early in the life of a specimen; thus, detection of a crack in a machine part does not necessarily mean that complete failure is imminent. In members in which a crack is caused by resonant vibration the crack could cover a large portion (easily greater than 50 per cent) of the gross area before "tuning-out" of the part occurs (see Appendix B) so that this effect may not protect the part from serious damage. Any observed changes in amplitude of resonant vibration of a member would likely indicate the presence of a fatigue

crack if the driving force is constant.

Positive mean stresses cause large increases in the rate of crack growth near the end of the life of a specimen. From this point of view it is more desirable to have a zero or negative mean stress.

Large stress amplitudes applied to parts in service should be avoided since fatigue crack growth appears to be proportional to a power of the range of applied stress. A small increase in the amplitude could cause a large increase in the rate of growth of an existing crack.

BIBLIOGRAPHY

1. Timoshenko, S.P., "History of Strength of Materials" McGraw-Hill Inc., 1953, pp. 162-172.

2. Moore, H.F., "A Study of Fatigue Cracks in Car Axles", University of Illinois Experimental Station Bulletin No. 165, 1927.

3. de Forest, A.V., "Rate of Growth of Fatigue Cracks", Journal of Applied Mechanics, Vol. 58, 1936, p. A23.

4. Orowan, E., "Theory of Fatigue of Metals", Proc. Roy. Soc., Series A, Vol. 171, 1939.

5. Bennett, J.A., "A Study of the Damaging Effect of Fatigue Stressing on X 4130 Steel", Proc. ASTM, Vol. 46, 1946, p. 693.

6. Head, A.K., "On the Growth of Fatigue Cracks", Philosophical Magazine, Vol. 44, 1953, pp. 925-938.

7. Weibull, W., "The Propagation of Fatigue Cracks in Light Alloy Plates", SAAB Aircraft Co. Tech. Note TN 25 (1954).

8. Weibull, W., "Effect of Crack Length and Stress Amplitude on Growth of Fatigue Cracks", Flygtekniska Forsoksanstalten Report 65, 1956.

9. Frost, N.E., and Phillips, C.E., "Studies in the Formation and Propagation of Cracks in Fatigue Specimens", International Conference on Fatigue of Metals, 1956, pp. 520-526.

10. Frost, N.E., and Dugdale, D.S., "The Propagation of Fatigue Cracks in Sheet Specimens", Journal of Mechanics and Physics of Solids, Vol. 6, 1958.

11. Liu, H.W., "Crack Propagation in Thin Metal Sheet under Repeated Loading", Trans. ASME, Series D, 1961, pp. 23-31.

12. Liu, H.W., "Fatigue Crack Propagation and Applied Stress Range", Trans. ASME, Series D, 1963, p. 116.

13. Paris, P., and Erdogan, F., Discussion of (15), Trans. ASME, Series D, 1963.

14. Hudson, M., and Hardrath, H.F., "Effects of Variable Amplitude Loading on Fatigue Crack Propagation Patterns", NASA TN D-1803, 1963.

15. Hudson, M., and Hardrath, H.F., "Effects of Changing Stress Amplitude on the Rate of Fatigue Crack Propagation in Two Aluminum Alloys", NASA TN D-960, 1961.

16. Weibull, W., "Further Investigations into Fatigue Crack Propagation in Sheet Specimens", Current Aeronautical Fatigue Problems, Pergamon Press, 1965.

17. Marin, J., "Mechanical Behavior of Engineering Materials", Prentice-Hall Inc., 1962, pp. 174-178.

18. Paris, P., and Erdogan, F., "A Critical Analysis of Crack Propagation Laws", Trans. ASME, Series D, 1963, pp. 528-534.

19. Lachenaud, R., "Fatigue Strength and Crack Propagation in AU2GN Alloy as a Function of Temperature and Frequency", Current Aeronautical Fatigue Problems, Pergamon Press, 1965.

20. Jacoby, G., "Observation of Crack Propagation on the Fracture Surface", Current Aeronautical Fatigue Problems, Pergamon Press, 1965.

APPENDIX A

TWO-STEP TESTS

A series of tests was conducted in which cracks were propagated to some selected value of L/b at a specific stress level and then the stress level was changed to some other value. The aim was to determine the effect of pre-stressing on the rate of crack growth at the second stress range (all tests had zero mean stress) and also to observe any delay in crack growth which might have occurred immediately following the change in the stress. Tests in which the second level of stress was greater than the first will be referred to as low-high tests; tests in which the second level was smaller than the first will be termed high-low tests.

Hudson and Hardrath (15) measured crack growth in axially loaded aluminum alloy specimens which were subjected to a single step in the loading program. It was found from a series of low-high tests that the rate of crack growth for both parts of the test was equal to that expected from corresponding portions of constant amplitude tests. However, when the second stress was less than the first (high-low tests) significant delays in crack growth were noted immediately after the change in stress level, if the decrement of stress was sufficiently large. Hudson and Hardrath attributed this to residual compressive stresses in the region of the crack

tip caused by the high stress. It was also observed that, once crack extension was resumed, it occurred at a rate equal to that for tests at a constant amplitude at this second stress.

Test Procedure

The tests were conducted using the cantilever test configuration previously used for Series A tests. Thus, in all tests the mean stress was zero. The apparatus and procedure were identical to those for the Series A tests except that a discrete step in the range of stress was made at an arbitrarily selected value of L/b of 0.3.

All of the curves presented in this section show the average crack growth found for the second level of stress.

High-Low Tests

Figure A.1 presents measured crack growth based on four tests in which the initial nominal stress range was $\pm$ 26 ksi and the second was $\pm$ 21 ksi. The dashed curve in the graph is the portion of Figure 4.2 for L/b greater than 0.3. When conducting this set of tests it was found that increases in crack length could be measured in 4,000 cycles after the change in stress level. Since the remaining life of these specimens at the time of the change in stress range was about 1.6×10^5 cycles, it was

concluded that no significant delay in crack growth occurred.

In a two-step test with $\bar{\sigma}_1 = \pm 35$ ksi and $\bar{\sigma}_2 = \pm 21$ ksi it was found that increases in the length of the crack could be measured in 2,000 cycles after the change in loading. As the remaining life would be of the same order as that in the previous test set, it was once again concluded that no significant delay in propagation occurred.

On the basis of these tests it appeared that the delay in crack growth noted by Hudson and Hardrath would occur only for very large decrements of stress.

Low-High Tests

Results of the low-high tests conducted are shown in Figure A.2 and A.3. In the tests shown in the former, the initial stress range was $\pm$ 26 ksi, followed by an increase to $\pm$ 35 ksi. Although there had been a wide range of scatter encountered in the constant amplitude test at $\pm$ 35 ksi, the results indicate that the rate of crack growth may have been greater in the two step test than in the corresponding portion of the constant amplitude test.

The fracture surface in the high stress portion of these tests did not display the transition phenomenon encountered in the single level tests. It was noted previously that this effect tended to cause decreases in the rate

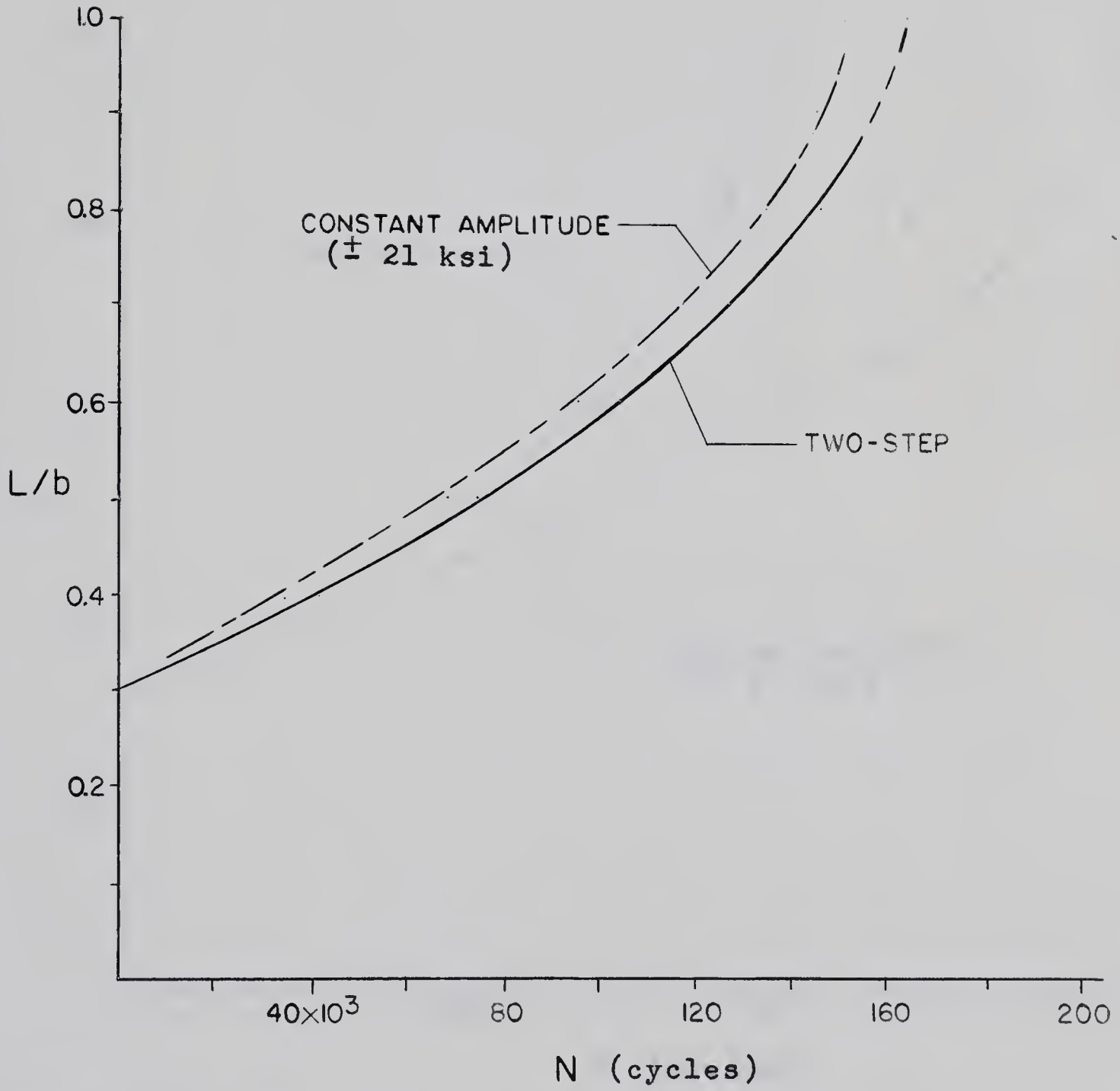

Figure A.1 Results of Two Step Tests with $\overline{\nabla_1} = \pm$ 26 ksi, $\overline{\nabla_2} = \pm$ 21 ksi

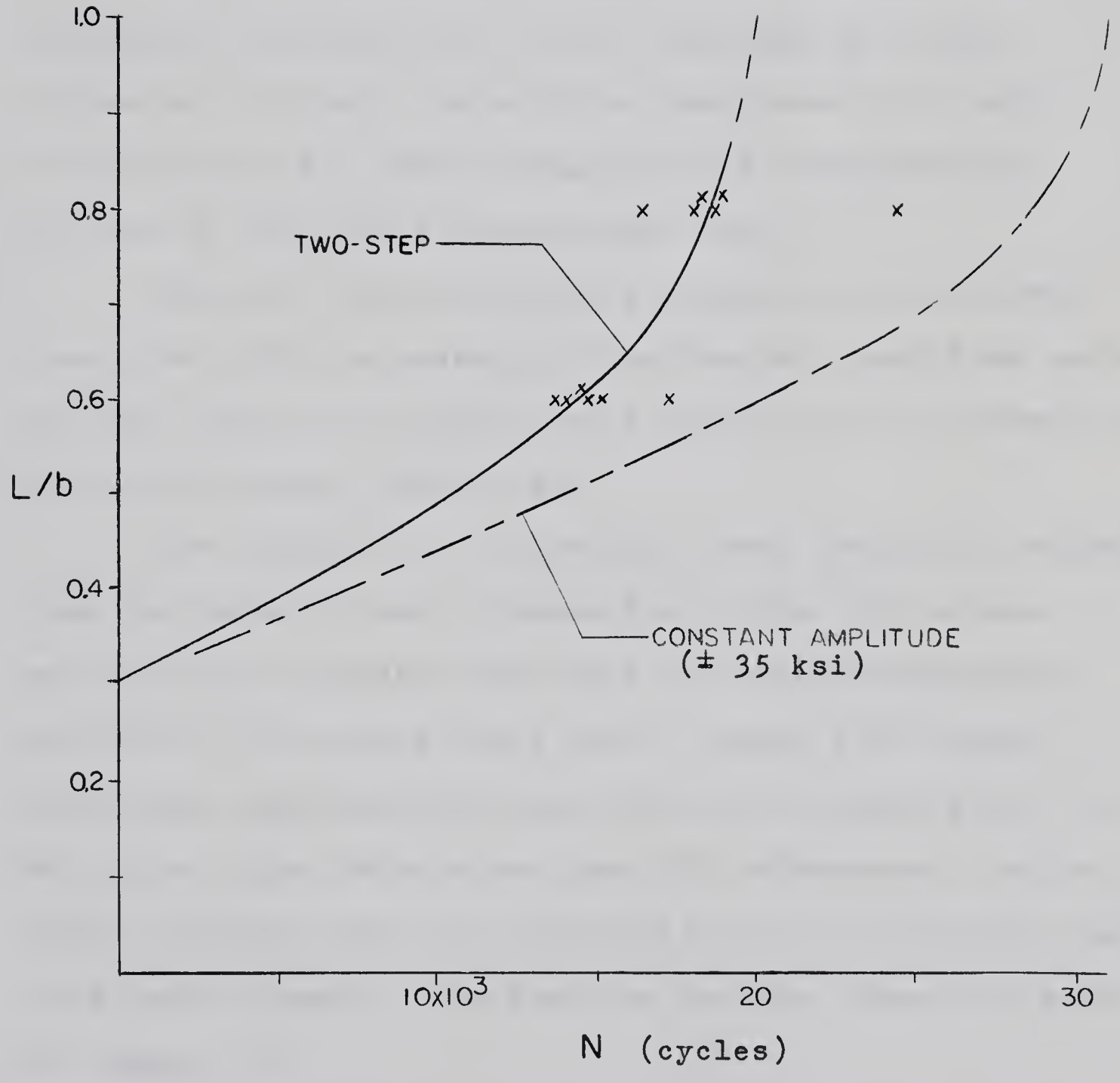

Figure A.2 Results of Two-Step Tests with $\overline{\sigma_1} = \pm 26$ ksi and $\overline{\sigma_2} = \pm 35$ ksi

of crack growth. This observation may explain the apparently greater rate of crack growth in the second part of these low-high tests as compared to the single level test at $\pm$ 35 ksi.

In the tests shown in Figure A.3 the crack was propagated initially at $\pm$ 21 ksi followed by a high stress of $\pm$ 26 ksi. As only two tests were run, individual curves are shown along with the corresponding portion of the single stress level test.

The two tests exhibited a greater rate of growth than that from the average of the constant amplitude tests; in fact, both of the tests had a greater rate of growth than any of the single level tests.

The results of the low-high tests conducted indicate that the rate of crack propagation in the high stress portion may be greater than that for the corresponding portion of the single level test. Jacoby (20) stated that other experimenters have found this result also, but he did not give details nor specific references. In the tests conducted here this increased rate of extension might have been related to the fracture surface transition noted in Chapter IV.

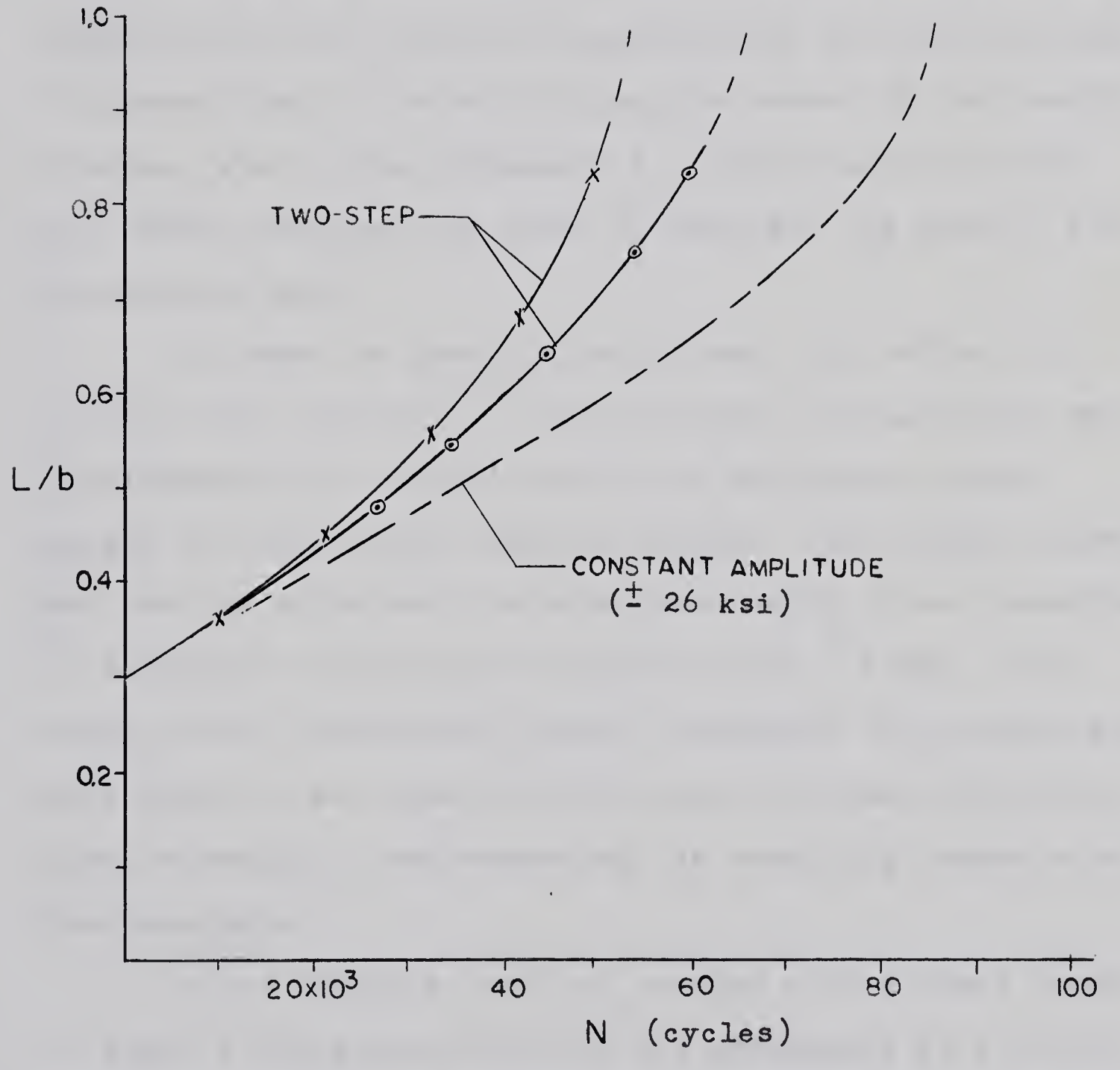

Figure A.3 Results of Two-Step Tests with $\overline{\nabla}_1 = \pm 21$ ksi and $\overline{\nabla}_2 = \pm 26$ ksi

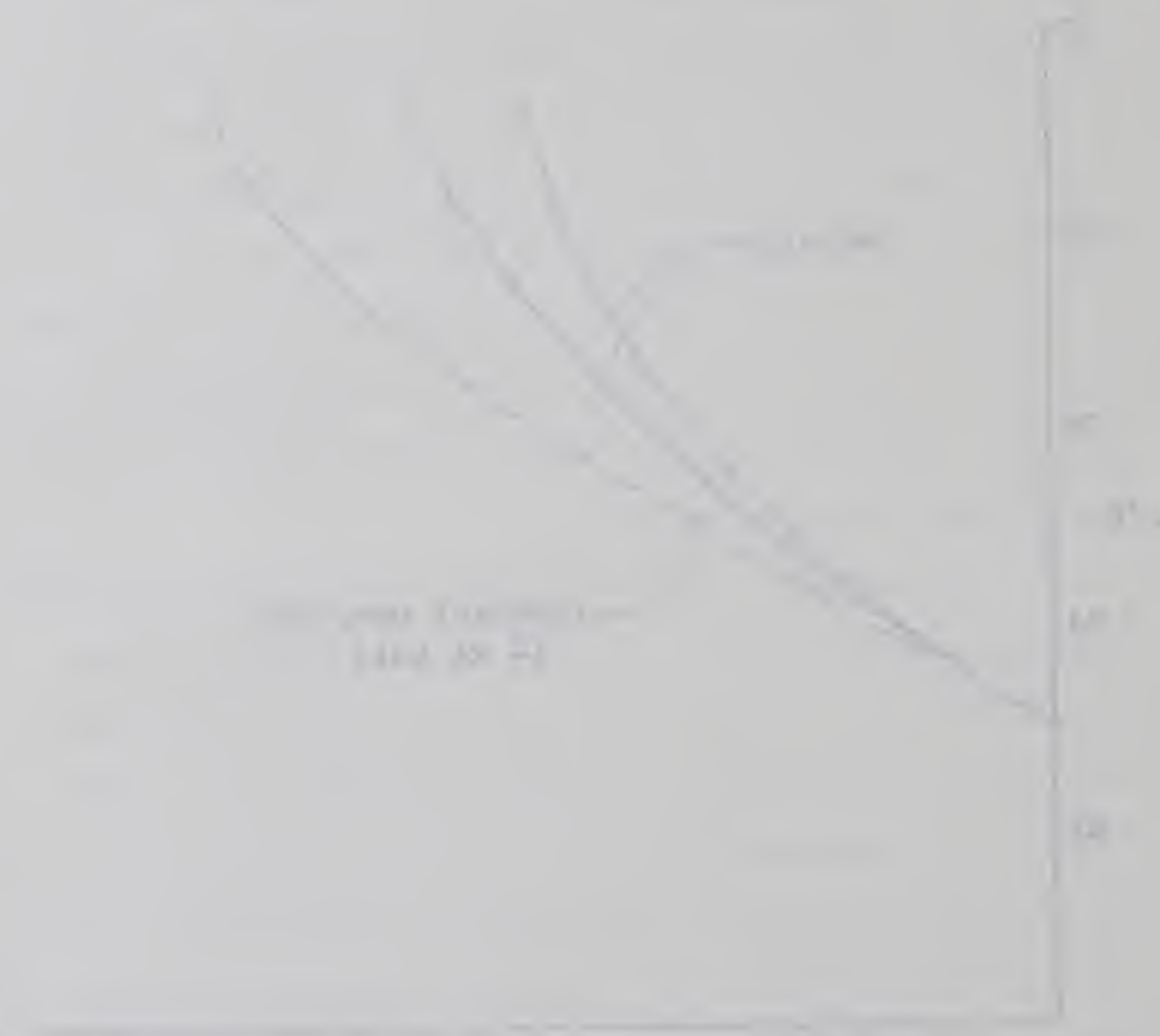

APPENDIX B

EFFECT OF LENGTH OF FATIGUE CRACK ON NATURAL FREQUENCY

Since the existence of a fatigue crack causes a reduction in the bending stiffness of a beam it is to be expected that the natural frequencies of the beam decrease. This was found to be true during the course of the testing program, when it was necessary to continuously decrease the shaker frequency in order to maintain the beam in its fundamental mode.

In order to quantitatively check this effect, a typical test specimen in the cantilever configuration was instrumented with bonded electrical resistance strain gauges to read dynamic bending strains. The bridge output was read on a Sanborn* recorder from which it was possible to determine frequencies to within about $\pm \frac{1}{4}$ cps. The value of the fundamental natural frequency of the beam was determined at any time by deflecting the beam statically, then releasing it and measuring the resulting response on the recorder.

After taking an initial reading with a crack length of zero, a crack was initiated and propagated at a stress range of $\pm$ 26 ksi. At intervals during the test the loading was interrupted and measurements of crack length and natural

* Dual Channel Carrier-Amplifier Recorder Model 321 manufactured by Sanborn Co.

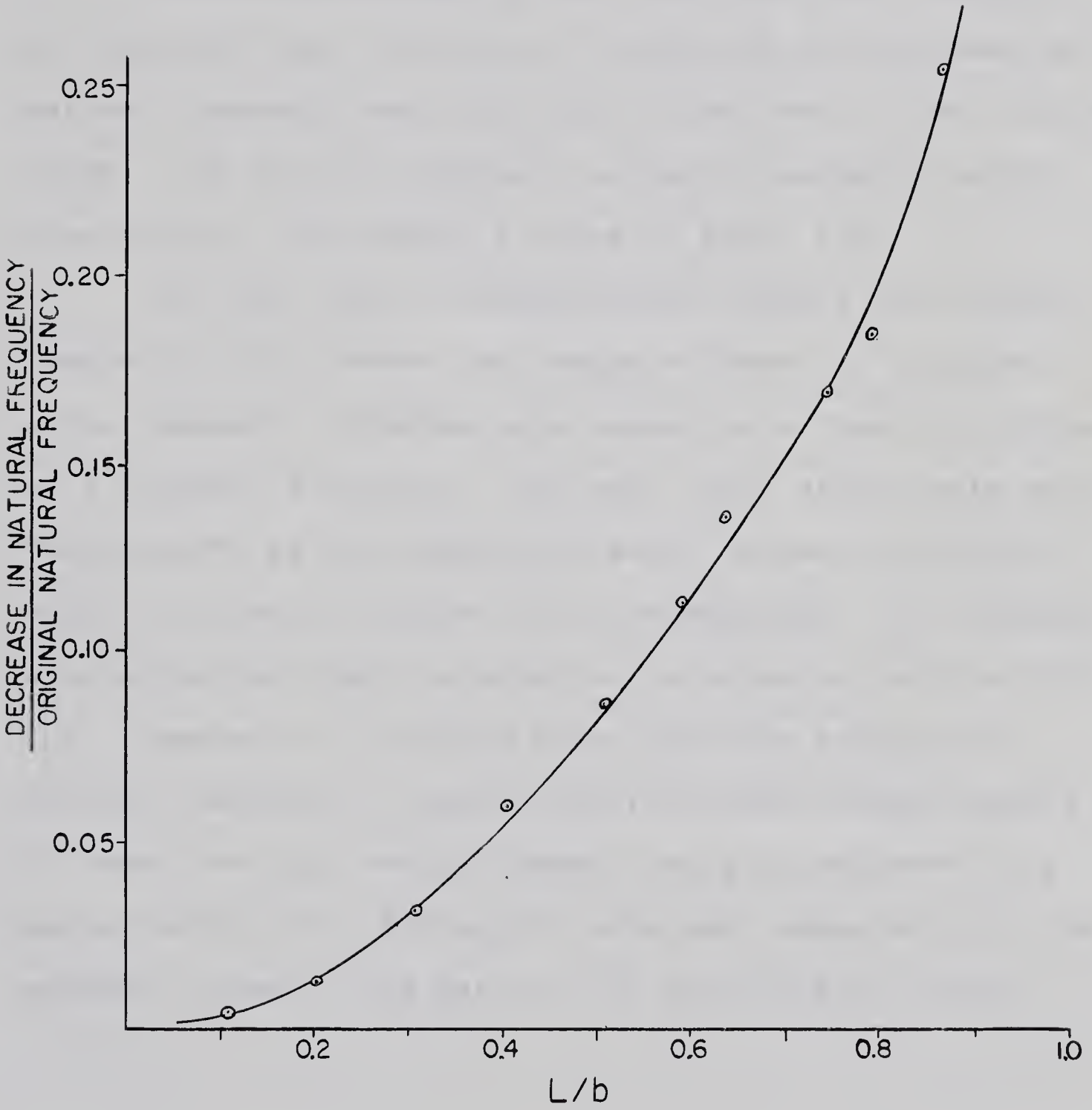

Figure B.1 Effect of Crack Length on Natural Frequency

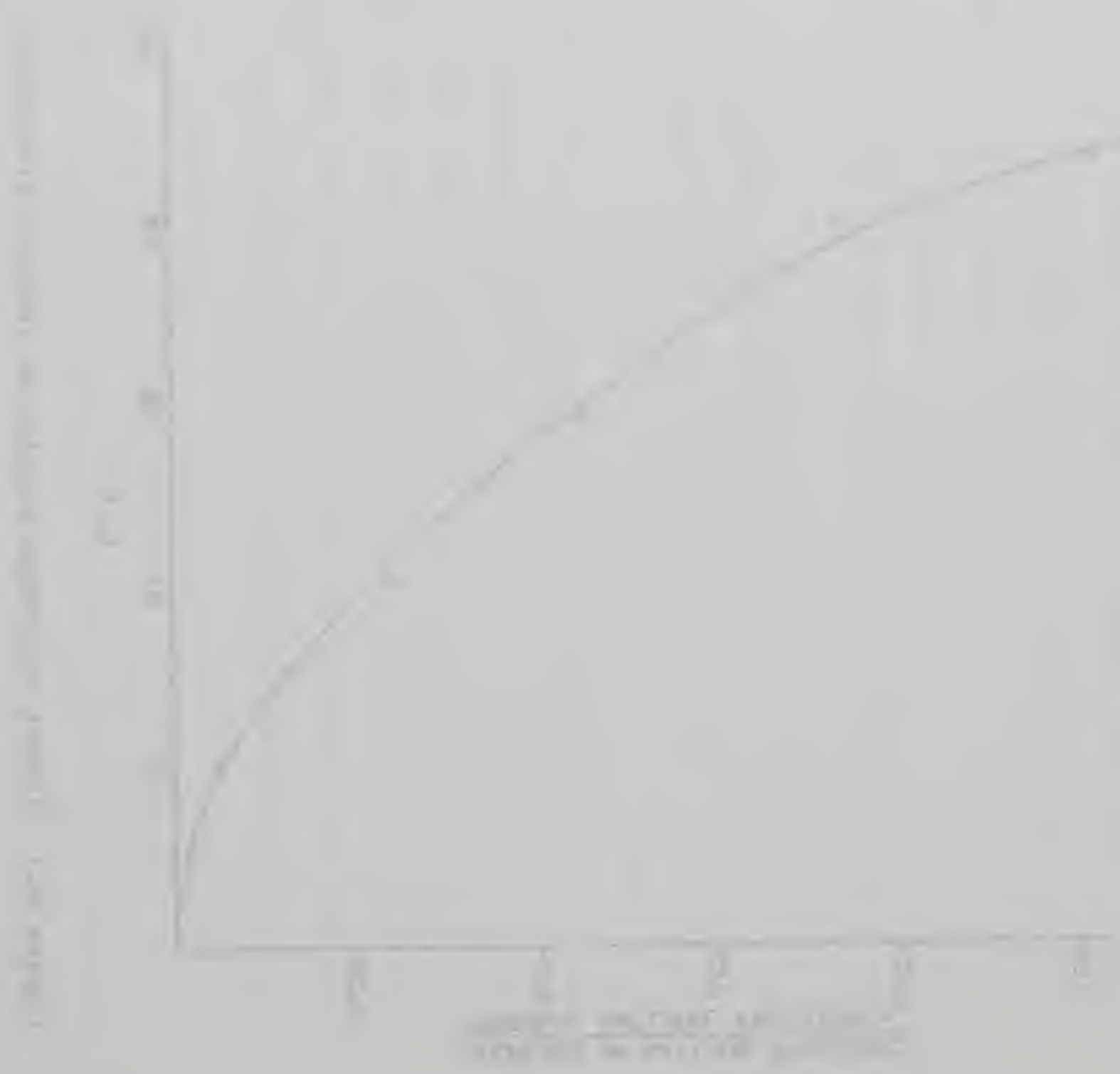

frequency taken. In this way the curve shown in Figure B.1 was obtained, where the results are presented in a dimensionless form.

It is interesting to note that when the original net area had been reduced by 50 per cent the decrease in natural frequency was only about 7 per cent of the original value. The natural frequency actually decreased rather slowly until L/b reached a value of about 0.8.

The fact that a fatigue crack reduces the natural frequency could reduce the damage suffered by a member where resonant vibrations are caused by a forcing function of a constant frequency. The part could effectively become "tuned-out", as the amplitudes would become sufficiently small to cause no further crack propagation. For example, this situation might be expected to arise in turbine blading. However, it is noted above that the decrease in natural frequency is small even for rather large lengths of crack, so that serious damage could be suffered by a member before this tuning-out occurred, especially if the response curve of the part is not particularly narrow.

APPENDIX C

DESCRIPTION OF TEST EQUIPMENT

Vibration Testing System

The vibration testing system employed throughout the test program was composed of an electrodynamic shaker and related equipment manufactured by the Unholtz-Dickie Corporation. A schematic diagram of the system is shown in Figure C.1.

The shaker itself was composed of an armature containing coils which carried an A.C. current, mounted inside of a D.C. field of fixed strength. The alternating current in the armature caused a cyclic force of the same frequency to be set up in the armature. The magnitude of this force was controlled by a gain adjustment on the power amplifier, while the frequency was the same as that of the controlling oscillator.

Adjustment of the power amplifier gain and the oscillator gave any desired acceleration, velocity or displacement of the shaker table at any frequency, within the limits of the machine. The armature, which was spring mounted to the shaker base, was capable of generating a peak force of 225 lbs . Thus, the maximum acceleration obtainable at any frequency depended on the combined mass of the armature and the mass carried by the table. When

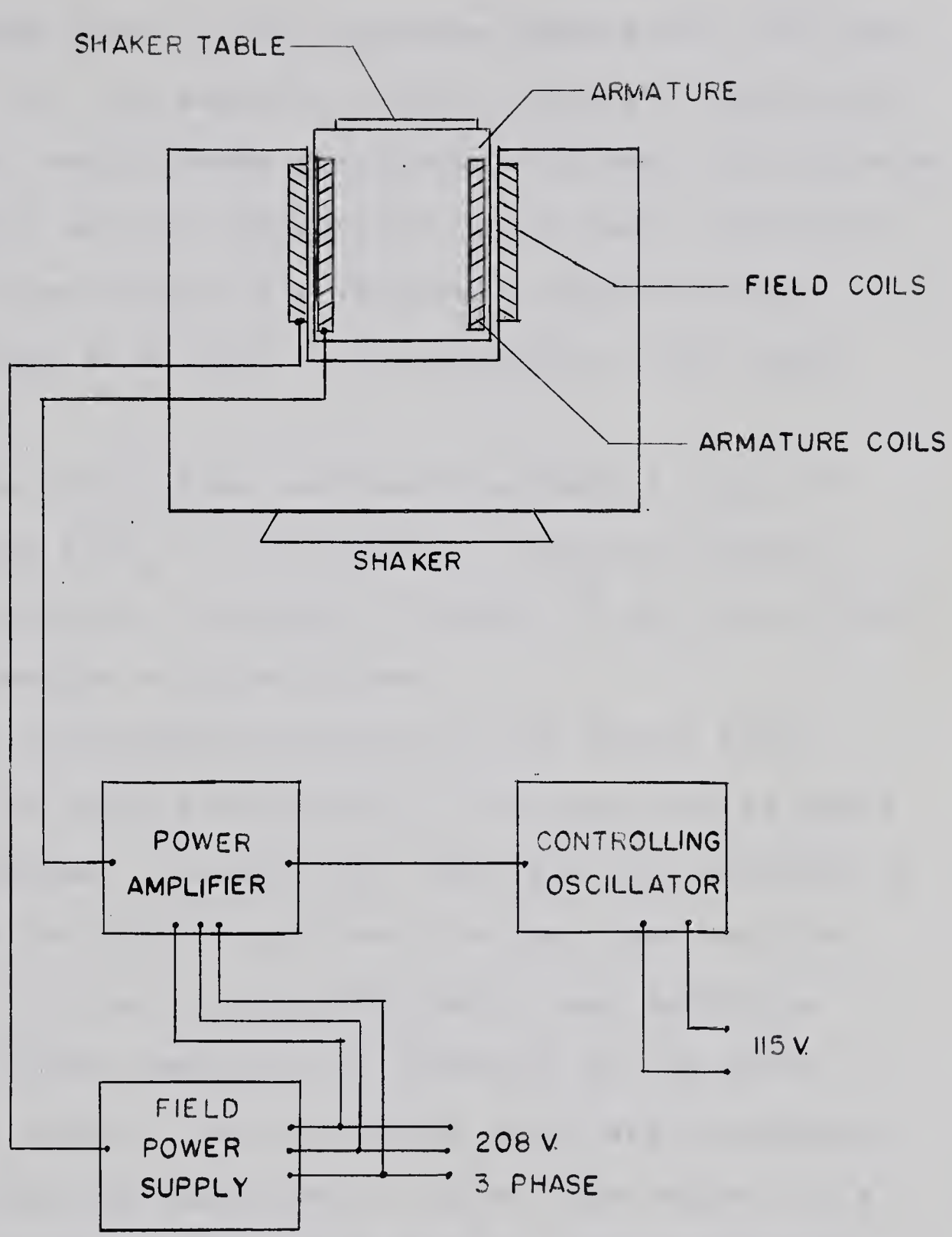

Figure C.1 Schematic Diagram of Vibration Testing System

the maximum force of the system was approached there was a danger that the amplifer output, which was normally a sine wave, would become distorted. Although the limits of the machine were not approached in the tests conducted, the amplifier output wave form was monitored on an oscilloscope as a check. No distortion of the output was noted.

The controlling oscillator allowed a range of frequencies from 5 to 60,000 cps. The test Series A was conducted at a frequency of about 60 cps while Series B was conducted at 100-120 cps.

An accelerometer mounted on the shaker table allowed the table acceleration to be monitored as tests were conducted. Knowing this value and the frequency of vibration the table displacement at any time could be checked. In the testing performed it was desirable to keep the double amplitude of vibration of the table to less than 0.20 in. so that little error was introduced in measuring the amplitude of the end (or centre) of a test specimen. It was found that the table amplitude did not exceed this value.

In conducting tests, the desired range of stress was obtained by setting the oscillator frequency at the natural frequency of the test specimen (by visual observation) and then adjusting the amplifier gain to obtain the proper amplitude of vibration of the test specimen.

Slip-Sync System

It was necessary to use a stroboscopic light when observing the amplitude of vibration of a test specimen so that the motion could be stopped at any time. For this purpose a device known under the trade name of "Slip-Sync"* was used. This is a frequency sensitive device which monitors some signal and outputs a signal to a strobe light at the same frequency as the monitored signal. In the test set-up used in this investigation the oscillator output signal was monitored by this device, so that the strobe light automatically operated at the same frequency as that of the test specimen.

The Slip-Sync also included a means to manually adjust the phase angle between the strobe light and the test specimen motion. This adjustment allowed viewing of the test specimen in any desired deflected position.

* Manufactured by Chadwick-Helmuth Co.